Geological Society, London, Special Publications

The Neogene to Recent Rallier-du-Baty nested ring complex, Kerguelen Archipelago (TAAF, Indian Ocean): stratigraphy revisited, implications for cauldron subsidence mechanisms

B. Bonin, R. Ethien, M. C. Gerbe, J. Y. Cottin, G. Féraud, D. Gagnevin, A. Giret, G. Michon and B. Moine

Geological Society, London, Special Publications 2004, v.234; p125-149.
doi: 10.1144/GSL.SP.2004.234.01.08

Notes

The Neogene to Recent Rallier-du-Baty nested ring complex, Kerguelen Archipelago (TAAF, Indian Ocean): stratigraphy revisited, implications for cauldron subsidence mechanisms

B. BONIN[1], R. ETHIEN[2,5], M. C. GERBE[2], J. Y. COTTIN[2], G. FÉRAUD[3], D. GAGNEVIN[4], A. GIRET[2], G. MICHON[2] & B. MOINE[2]

[1]*UPS-CNRS-FRE 2566 'Orsayterre', Département des Sciences de la Terre, Université de Paris-Sud, F-91405 Orsay Cedex, France (e-mail: bbonin@geol.u-psud.fr)*

[2]*CNRS-UMR 6524 'Magmas et volcans', Département de Géologie-Pétrologie-Géochimie, Université Jean-Monnet, F-42023 Saint-Etienne Cedex 2, France*

[3]*CNRS-EP 125, Département des Sciences de la Terre, Université de Nice – Sophia Antipolis, F-06108 Nice Cedex, 2 France*

[4]*Department of Geology, University College Dublin, Belfield, Dublin 4, Eire.*

[5]*GEMOC, Macquarie University, Sydney, Australia*

Abstract: The Kerguelen Archipelago is made up of a stack of thick piles of Tertiary flood basalts intruded by transitional to alkaline igneous centres at various times since 30 Ma ago. In the SW, the Rallier-du-Baty Peninsula is mostly occupied by two silicic ring complexes, each with an average diameter of 15 km, comprising dissected calderas cross-cut by subvolcanic cupolas. Previous radiometric determinations yield ages ranging from 15.4 to 7.4 Ma in the southern centre, and 6.2 to 4.9 Ma in the northern one. The felsic ring dykes were injected by coeval mafic magmas, forming, successively, swarms of early mafic enclaves, disrupted synplutonic cone sheets, and late cone-sheets. After the emplacement and subsequent unroofing of the plutonic ring complexes, abundant and thick trachytic pyroclastic flows and falls were emitted from the younger caldera volcanoes, while hawaiite and mugearite lava flows were erupted from marginal maars and cones. Huge trachyte ignimbritic flows filled the glacial valleys in the central Peninsula, and capped lacustrine deposits and older lava flows, while related pumice falls are widespread throughout the archipelago. This powerful plinian eruption took place after the network of glacial valleys was established, but before the Little Ice Age that occurred during the last centuries. In the south of the peninsula, even younger trachytic formations are exposed, and fumarolic vents are still active.

The growth mechanisms of a caldera-related ring complex can be explained as a repetitive sequence of two eruptive episodes. The first episode of hydrofracturing, induced by volatile exsolution within the evolving magma chamber, creates a vertical circular fracture zone, along which highly vesiculated magmas are emitted during explosive eruptive events occurring at the surface in a caldera volcano. It is followed by a second episode of cauldron-subsidence of a crustal block down to the degassed magma chamber, induced by pressure release. Downward movement of the crustal block favours the emplacement at shallow depths within the older caldera-filling formations, of discrete magmatic sheets characterized by a 16-km mean diameter and a 1-km mean thickness, corresponding to an average unit volume of 200 km^3. Actually, the estimated volumes of the different igneous episodes within the Rallier-du-Baty nested ring complex vary from 60 to 900 km^3, and correspond to the production during 15 Ma of about 2800 ± 850 km^3 of new materials and a net crustal growth of about $100 \pm 30 \times 10^3$ m^3 per year.

Introduction

In the twentieth century, caldera-related ring complexes were the subject of numerous studies. These were initiated by the seminal paper of Clough *et al.* (1909) on the district of Glen coe, Argyllshire, Scotland, where, for the first time, they describe a cauldron, in the sense of an eroded caldera with inverted relief, formed by subsidence having affected an area, roughly oval in shape, delineated by a boundary fault. Observing that uprise of a series of marginal intrusions accompanied the subsidence, they suggest that these intrusions could have been

From: BREITKREUZ, C. & PETFORD, N. (eds) 2004. *Physical Geology of High-Level Magmatic Systems.* Geological Society, London, Special Publications, **234**, 125–149. 0305-8719/04/$15.00

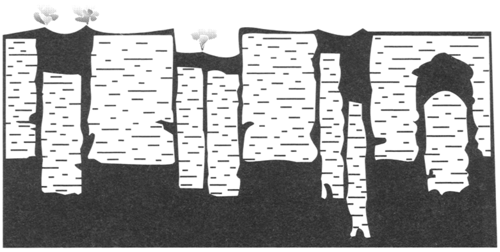

Fig. 1. The original concept of cauldron subsidence, as redrawn from figure 14 in Clough *et al.* (1909).

related to subterranean foundering, favouring the emplacement of shallow plutons resembling bell-jars in form (Fig. 1).

The cauldron-subsidence hypothesis was subsequently validated by Richey who interpreted the Mourne Mountains, Northern Ireland (Richey 1928) and afterwards the intrusives (Richey 1932) of all the British Volcanic Tertiary Province (Richey 1935) as ring complexes, most of them emplaced within a coeval volcanic blanket. Anderson (1936), on the same vertical axis, related caldera volcanoes and plutonic ring complexes, and offered the first mathematical theory based on fluctuating magmatic pressure within a deep magma chamber, parabolic in form. The 1930s saw the discovery of numerous ring structures throughout the world (e.g. Kingsley 1931; Bain 1934), so that, since then, cauldron subsidence-related ring complexes have been defined a worldwide class of intrusive plutons (Billings 1943, 1945; Bonin 1986).

From a structural point of view, ring complexes share some characteristics with laccoliths, e.g. their diameters (7–15 km) and thicknesses (0.5–1.0 km) plot in the laccolith field of McCaffrey & Petford (1997), defined by $T = 0.12\ L^{0.88}$, where T is the thickness, L the length, 0.12 a constant, and 0.88 (±0.10) the power-law exponent. Taking into account the circular shape of ring complexes, the relationship becomes $T = 0.22\ R^{0.88}$, where R is the radius. However, ring complexes differ from laccoliths by having steeply outward-dipping to subvertical cylindrical, not rectilinear, feeder zones, and by providing space by floor subsidence rather than by floor lifting. The dimensional similarity, defined by $T = bL^a$ with $a < 1$, shared by sills, laccoliths and plutons (Cruden & McCaffrey 2001) with ring complexes, suggests that they form by similar processes.

The Rallier-du-Baty ring complex, Kerguelen Archipelago, is located within an oceanic island on top of a plateau characterized by a 22-km thick oceanic crust (Charvis *et al.* 1995). Abundant field evidence, such as intrusive contacts, chilled margins, xenoliths and screens of country rocks, contact aureoles, etc., was collected during summer expeditions. Like the typical ring structures emplaced in the continental crust, the Rallier-du-Baty igneous complex is made up of several discrete intrusions, associated with coeval volcanic formations. As such, it provides a good area for testing, in an oceanic environment, the current models of pluton emplacement by lateral spreading and self-affine inflation. This paper evaluates the feasibility of the different growth mechanisms by reviewing the field evidence and by assessing how space was created at very shallow depths within the crust.

The Rallier-du-Baty nested ring complex: geodynamic settings

In the Indian Ocean, the Kerguelen Plateau and Broken Ridge were originally contiguous and split off 46–43 Ma ago (Munschy *et al.* 1994, and references therein). Their estimated combined crustal volume of approximately 57×10^6 km^3 is comparable to the Ontong Java Plateau in the Pacific – the largest documented oceanic plateau on Earth (Schubert & Sandwell 1989). Located within the Antarctic plate, the 2000-km long and 200–600-km wide Kerguelen Plateau is located at latitudes between 46 and 64°S and its mean altitude is 2000 to 4000 m higher than the neighbouring oceanic basins (Schlich 1994).

The Kerguelen Archipelago (6500 km^2) (Giret 1993) is the third largest oceanic island after Iceland and Hawaii (Giret *et al.* 1997). It is located at the northern tip of the Kerguelen Plateau at latitudes 48–50°S and longitudes 68.5–70.5°E (Fig. 2). Mont Ross, its highest point, culminates at 1850 m above sea-level. The Rallier-du-Baty Peninsula, with an area of approximately 800 km^2, corresponds to 12% of the emergent land.

A brief overview of the Kerguelen Archipelago

Coarse-grained intrusive rocks represent a significant proportion of the archipelago, currently covering an area of about 8% of the land, whereas finer-grained intrusive rocks correspond to about 7% and volcanic, dominantly basaltic, units occupy 85% (Nougier 1970). Plutonic and volcanic rocks yield identical isotopic ratios (Dosso *et al.* 1979; Dosso & Murthy 1980)

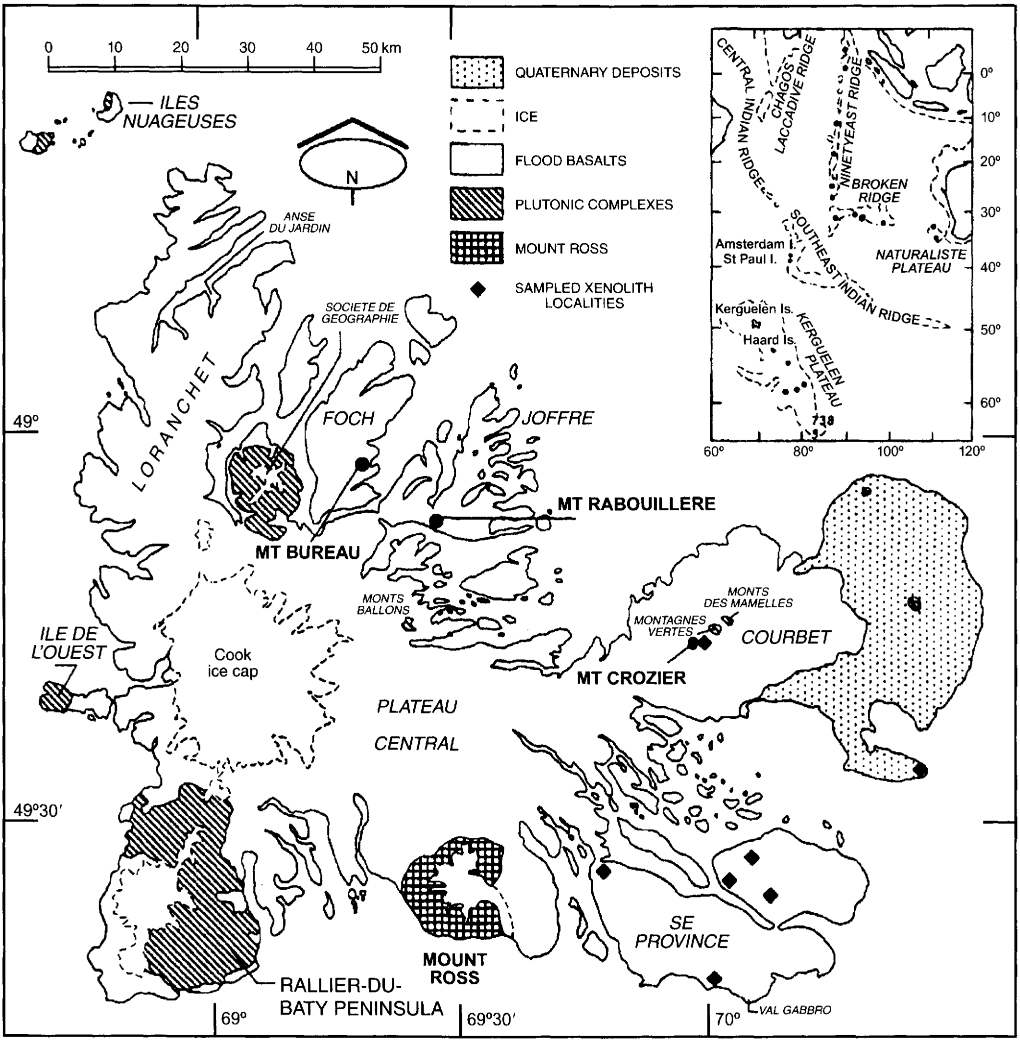

Fig. 2. Map of the Kerguelen Archipelago, showing the location of the Rallier-du-Baty Peninsula and the major features of the main island (after Gagnevin *et al.* 2003). Diamonds: localities where lower crust xenoliths were sampled (Gregoire *et al.* 1998); dots: localities where stratigraphic sections of flood basalts were extensively sampled. Inset: position of the Kerguelen Archipelago within the Indian Ocean; dots: drilling and dredging sites.

and no significant evolution of the source composition is recorded for the the last 30 Ma (Yang *et al.* 1998). The igneous complexes were emplaced within older flood basalts and are cross-cut or capped by younger pyroclastic and lava flows. Their sizes vary from as little as 1 km, up to 18 km. The available radiometric ages range from 39 to 0.13 Ma (Giret 1990; Weis *et al.* 1998), although younger age determinations are expected (work in progress). The largest igneous complex (about 80% of the intrusive rocks) is located in the Rallier-du-Baty Peninsula, in the SW of the archipelago (Fig. 2).

Previous work on the Rallier-du-Baty igneous complex

After the first study of an aegirine-bearing syenite by Lacroix (1924), the large extension of syenite and granite was observed and mapped by Aubert de la Rue (1931) and Nougier (1970).

The plutonic complex, involving a suite of gabbro, diorite, syenite and granite, cross-cuts Tertiary basalt lava flows and is covered by Quaternary basic to felsic volcanic formations (Marot & Zimine 1976; Lameyre *et al.* 1981). K–Ar and Rb–Sr isotopic studies in plutonic rocks document ages ranging from 15.4 to 4.9 Ma, short-lived magmatic processes and a pure mantle signature (Lameyre *et al.* 1976; Dosso *et al.* 1979). Combined field and laboratory works during the first half of the 1970s resulted in a geological map at the scale of 1:50 000 of the Rallier-du-Baty Peninsula (Giret 1980), where five discrete intrusive centres are distinguished and labelled (Fig. 3), according to their geographical position, as southern (S), intermediate (I), western (W), northern (N) and northeastern (NE).

From 1976 to 1994, no supplementary field studies were performed on the peninsula. As glaciers and ice sheets throughout the archipelago are currently being subjected to protracted reduction, new clean exposures have been revealed, and a reassessment of the geological map of the northern part of the Rallier-du-Baty Peninsula was unavoidable. A 400-km^2 area south of the Cook ice sheet, corresponding to one-half of the peninsula, was systematically surveyed during the CARTOKER 94–95 summer expedition in order to provide an updated field-controlled map (Fig. 4). CARTOKER is an acronym for 'Cartographie de Kerguelen', which means Kerguelen Mapping.

The Rallier-du-Baty nested ring complex: field notes

Country rocks

The country rocks are made up of an extensive pile of flood basalts that have suffered extensive zeolite alteration. Early Miocene minimum ages are suggested by the 15 Ma maximum age determined for the zeolitization event (Giret *et al.* 1992). In the nearby Mont Ross area, the unaltered feeder dykes of flood basalts yield K–Ar conventional ages of 24–20 Ma (Weis *et al.* 1998). The whole of the volcanic pile could not be observed: the lower units being hidden under the sea. About 1000 m thickness of flood basalts can be observed. Two discrete sequences are displayed:

1 The lower sequence forms small hills above the sea and around the large, flat valleys. Lava flows and associated breccias fill up a dense network of channels. The 200-m thick section displays, from bottom to top:
   - a 150-m thick series of 5- to 10-m thick basaltic lava flows, with rough columnar jointing. In each lava flow, emplacement within shallow water is indicated by a brecciated lower zone with clasts decreasing in size from 4 cm at the base to 0.5–0.2 mm to the top, overlain by an aphanitic upper zone containing 1-mm to 5-cm wide vesicles, filled or unfilled with late-stage minerals, indicating rapid degassing and air-cooling.
   - 0.5- to 1.5-m thick breccias, intercalated in places among lava flows. Scoriaceous bomb fragments provide evidence of renewed volcanic activity after a period of quiescence.
   - a 50-m thick chaotic breccia, completing the sequence. It contains a package of metre-scale lava tongues, scoriaceous bomb fragments, some of them with a rounded shape, and lapilli, set within a palagonitic lapilli–ash matrix, suggesting aerial explosive volcanic eruption and emplacement in shallow water.

2 The more monotonous upper sequence forms high plateaux and summits, including the base of the Cook ice sheet. The *c.* 800-m thick series is composed of a number of extensive 15–20-m thick lava sheets, covering areas of more than 100 km^2. In this part of the archipelago, outpouring of lava flows occurred at or above sea-level. Intercalated 0.1–0.5-m thick red layers correspond to hydrothermally altered vitreous ash falls (Bellair *et al.* 1965). Breccias and conglomerates with up to 30-cm diameter boulders are exposed at various levels of the sequence. They were derived from nearby high ground and deposited during periods of volcanic quiescence and erosion.

Vertical dykes and associated horizontal sills were observed locally in the two sequences of the flood basalt pile. Their average widths are less than one metre, and their basaltic composition is identical to that of the lavas. They are, therefore, considered as feeder conduits of the overlying flows and sheets.

Lavas are aphanitic alkali basalt, subsequent alteration is evidenced by late crystals growing in vugs and vesicles. Silica minerals (quartz, chalcedony, and/or opal), and calcite are invariable components of the hydrothermal association, while adularia and celadonite are less widespread. A regional-scale zeolitization event affected the archipelago 15–12 Ma ago (Giret *et al.* 1992). A heulandite–scolecite–stellerite–stilbite zeolite assemblage was observed in the SE of the

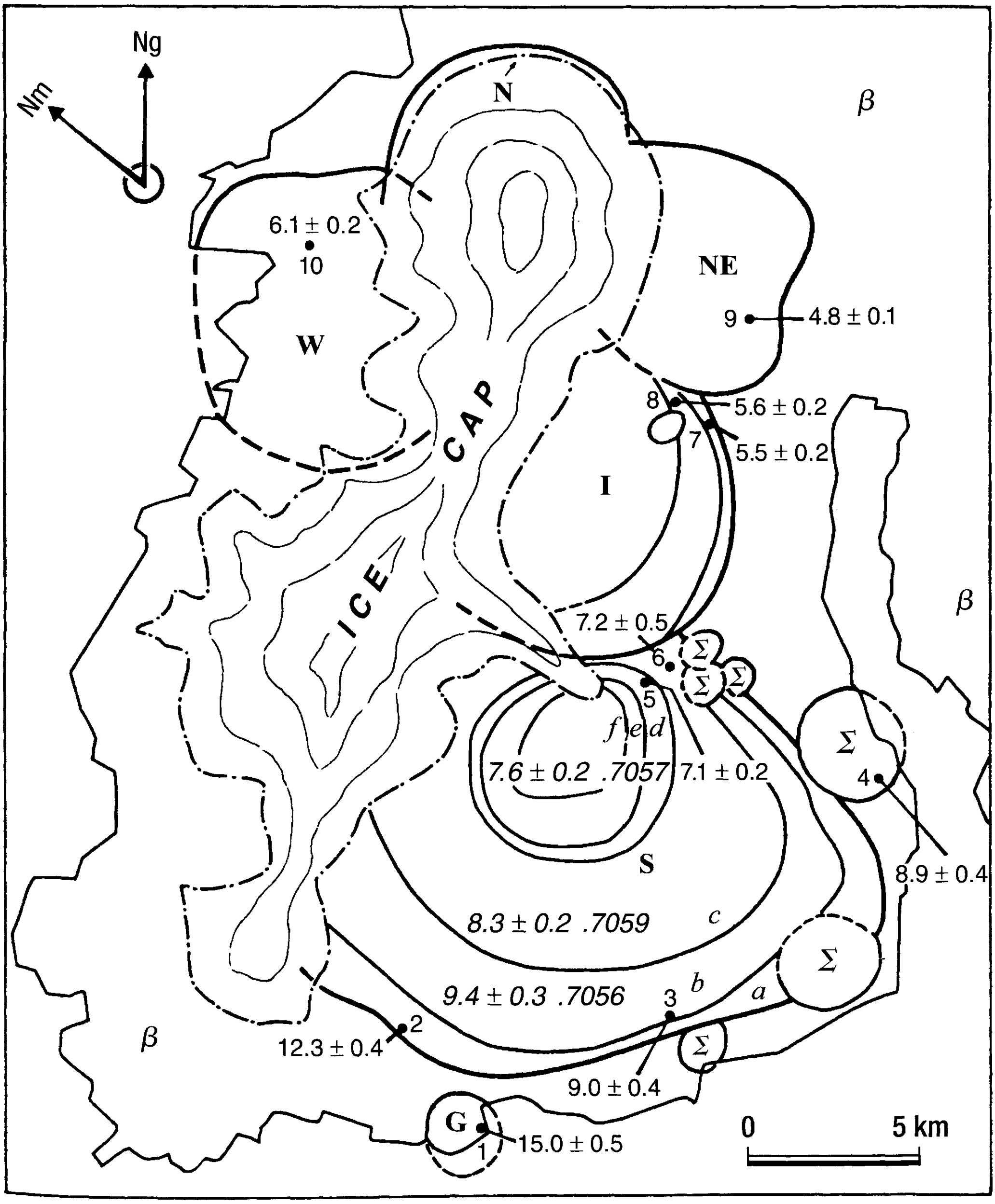

Fig. 3. Preliminary sketch map of the Rallier-du-Baty nested ring complex identifying S, I, NE, N and W massifs, and isotopic data (after Lameyre *et al.* 1976): numbers in italics, Rb–Sr isochron method; other numbers, sampling localities and K–Ar conventional method. Nm, magnetic North; Ng, geographical North. In the southern ring complex: β, basalt; G, gabbro; Σ, syenite satellite cupolas; *a*, *b*, *c* and *d*, syenite–granite units 1, 2, 3 and 4; *e* and *f*, assumed inner units (see text).

Cook ice sheet (Verdier 1989). Estimated temperatures of 110 to 180 °C versus burial depths of 1600 to 2500 m identify high thermal gradients of 70 to 100 °C km^{-1}.

This event was followed locally by the thermal event induced by the emplacement of the Rallier-du-Baty igneous complex itself. No zeolites remain in vugs and vesicles within a 3-km

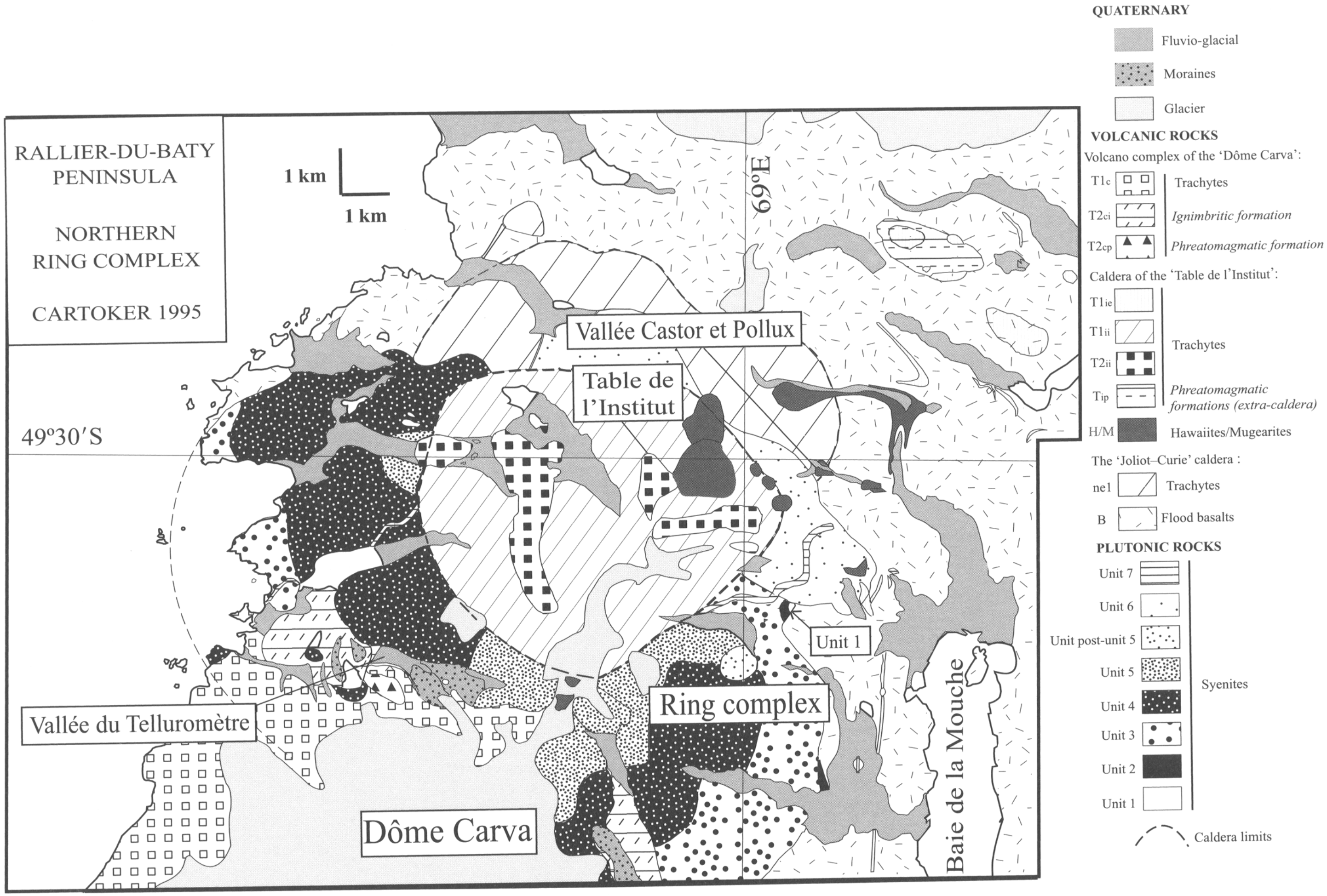

Fig. 4. Geological map of the northern ring complex, as identified during the CARTOKER 94–95 resurvey (slightly modified after Gagnevin *et al.* 2003).

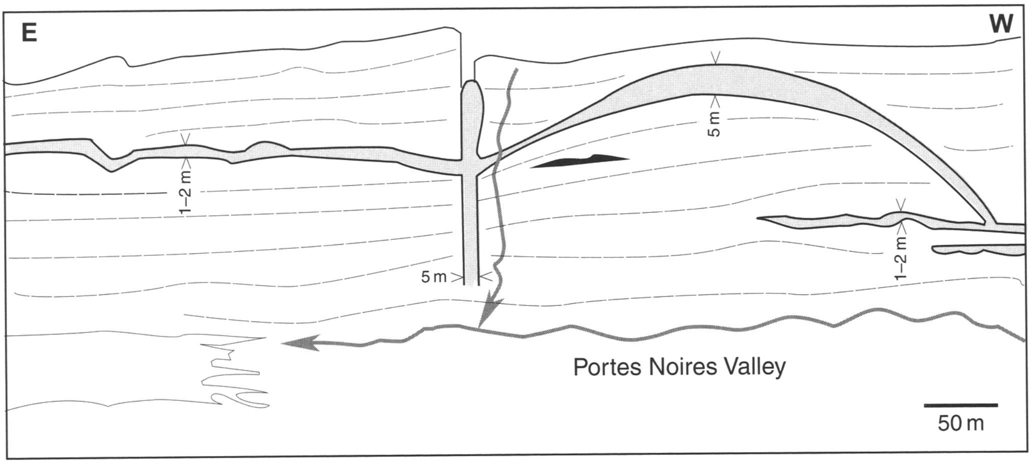

Fig. 5. Sketch of the dyke-and-sill network, on the right side of the Portes Noires Valley (Bonin 1995, unpublished). A dyke is related to curved and jumping sills of trachytic composition (in grey). A smaller sill is made up of obsidian (in black).

wide contact aureole, which is constituted by three zones:

1 the outer zone is characterized by the greenschist-facies association at 3 km to 600 m away from the contact;
2 the middle zone is marked by the albite–epidote hornfels facies association at 600 to 100 m away from the contact;
3 the 100 m-wide inner zone is occupied by the amphibole-hornfels facies. A basalt sampled at 30 m from the contact of the southern centre yields a K–Ar thermal reset age of 11.5 ± 0.2 Ma (Nougier 1970).

External trachytic domes and associated pumice deposits

In the SE of the Cook ice sheet, rounded summits culminating at about 600 m above sea-level are occupied by 0.8- to 2.5-km wide domes of slightly porphyritic trachyte. The volcanic structures were built by a series of contrasting eruptive styles. The early hydro-plinian to plinian episodes resulted in the deposition of thick pumice tuff and breccia rings and ended with the emplacement of multiple extrusions capped by a 250–300-m high main dome. Tuff rings are composed of inward-dipping stratified deposits, composed of white to light-yellow centimetre-scale trachyte pumice, black 1–2-cm wide obsidian balls, and 5-cm wide basalt fragments, set within an ash matrix, and occasionally of breccias composed of volcanic bombs. Well-defined horizontal lamination and vertical columnar jointing indicate that domes were emplaced in highly viscous and even rigid states, and cooled very slowly. A loose network of dykes and sills corresponds to the feeder conduits of the trachyte domes (Fig. 5). North–South-trending 5-m thick dykes and 1- to 5-m thick sills are filled with porphyritic trachyte, while narrower (30–40-cm thick) sills are filled with vitreous rhyolite (Gagnevin *et al.* 2003). Although the eruption ages are unknown, the well-preserved primary volcanic features suggest relatively recent ages.

Centimetre- to decimetre-thick reworked pumice deposits partly fill in valleys and low relief to the east. The primary air-fall deposits driven by westerly winds were removed later on by snow and water. As these deposits are more abundant and thicker at the vicinity of trachytic domes, they are likely to have been derived at least partly from the early plinian episodes. A blanket of pumice deposits of unknown age covers all of the Kerguelen archipelago.

The southern ring complex

The intrusive centre S, the best known, provides an example of a classical ring complex, with ring dykes and satellite intrusions intercalated with screens of older basalt. The central part is occupied by large glacial valleys, lowlands and flat hills, culminating at 549 m above sea level. The border zones constitute an amphitheatre of crests with elevations up to 865 m above sea-level. Access to the area is easy through sandy bays and large breaches opened by Quaternary glaciers. The formations are well exposed on cliffs and hills.

Field evidence was examined in detail during summer expeditions from the 1950s to the 1970s and resurveyed during the CARTOKER 94–95 summer expedition. One single ring complex is identified, constituted by large ring dykes, arcuate dykes and small cupolas aligned along the boundary fault (Fig. 4). Its elliptical outline is defined by a 17-km long east–west major axis and a 15-km long north–south minor axis (Marot & Zimine 1976; Lameyre *et al.* 1981). The Rb–Sr ratios display such a large range of values that the whole-rock Rb–Sr isochron method can be used successfully for age determination of at least three ring dykes, supplemented by K–Ar ages (Lameyre *et al.* 1976; Dosso *et al.* 1979).

Early composite intrusions Two 1.5–2.0-km wide composite intrusions are exposed on the southern side of the complex. At the contact, basaltic wallrocks dip 20–30° southwards and are brecciated by aplitic injections. A bimodal association of gabbro and syenite, each end-member occupying 10–15% of the area, is accompanied by a compositionally expanded monzogabbro–monzodiorite–monzonite hybrid suite, where mafic enclaves of two size ranges: 1–10 m and 50–100 m, are set within a felsic matrix. The oldest rock of the ring complex is the Anse du Gros Ventre gabbro, as shown by K–Ar ages of 15.4 ± 0.5 Ma on whole rock and 13.6 ± 0.4 Ma on biotite (Dosso *et al.* 1979).

Plutonic ring dykes In the 1:50 000 geological map of the centre S (Giret 1980) eight ring dykes, four late arcuate dykes and two types of satellite cupolas are indicated. From the re-appraisal of field evidence during the 1994–1995 summer expedition, the number of ring dykes was reduced from eight to four. Ring dykes are numbered hereafter from 1 to 4 from older to younger, i.e. from the rim to the core of the igneous intrusion.

1 The hypersolvus alkali-feldspar quartz-syenite unit 1 is directly at the contact with the basalt country rocks. Its preserved thickness ranges from 200 m up to 500 m. In the 50-m thick marginal zone, the texture is porphyritic, with alkali-feldspar megacrysts, and two types of enclaves of wallrocks are exposed: metre-scale rounded blocks occur at 30 m from the contact, whereas smaller, but angular, blocks at only 1–2 m from the contact show no signs of rotation and show limited stoping effects. The rest of the ring dyke is occupied by a coarser-grained rock. The K–Ar age of 12.6 ± 0.4 Ma is consistent with the Rb–Sr isotope data.
2 The hypersolvus alkali-feldspar quartz-syenite unit 2 is exposed inside and topographically below the unit 1. Its observed thickness ranges from 200 to 500 m. Along the contact, hectametre-scale disrupted screens of basalt are locally preserved. Elsewhere, unit 2 yields a marginal aplitic facies enclosing 0.5–1.0-m elongated enclaves of quartz syenite of unit 1. The Rb–Sr age of 9.7 ± 0.2 Ma substantiates a *c.* 2.9-Ma period of quiescence between the emplacement of units 1 and 2. A late aplitic dyke yields a consistently lower K–Ar age of 9.2 ± 0.4 Ma.
3 The hypersolvus alkali-feldspar quartz-syenite unit 3 is the most extended intrusion. Its roof has been removed by erosion and its floor by the later ring intrusion, so that its thickness is unknown, but could have exceeded 600 m. At the contact with unit 2, a marginal fine-grained facies has been identified in some places. Mafic (microgabbro) and felsic (trachyte) dykes and cone sheets constitute characteristic features. A Rb–Sr age of 8.6 ± 0.1 Ma substantiates a *c.* 1.1-Ma period of quiescence between the emplacement of units 2 and 3.
4 The heterogeneous unit 4 encompasses hypersolvus alkali-feldspar quartz syenite to granite rock types. It occupies the central part of the southern ring complex. Its total thickness could exceed the 500 m observed on the cliffs.

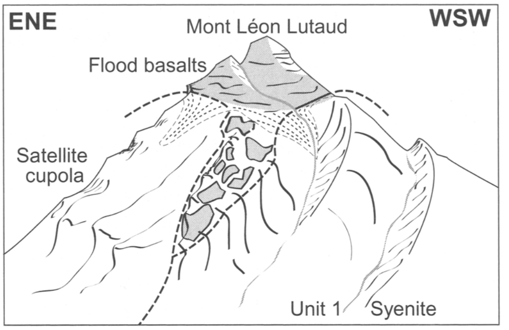

Fig. 6. Relationships between Neogene flood basalts (in grey), unit 1 syenite of the southern ring complex and Anse Syenite satellite cupola (both in white). Note the brecciated aspect of the basaltic screen between the two intrusions (after a sketch by Marot & Zimine 1976).

The outer contact with unit 3 is almost vertical, with angular outlines, and turns horizontal some 50 m below the Les Deux Frères summit. Within

500 m of the contact, the quartz syenite of unit 3 is hydro-fractured and forms breccias with 10-cm blocks of altered syenite set within a 2-cm wide dark-green aplitic matrix. Blocks of alkali-feldspar quartz syenite of unit 3 have been converted into a secondary fenite assemblage, while the dark aplitic matrix is rockallite, characterized by aegirine needles. The marginal facies of unit 4 is highly oxidized, with joints coated with bluish oxides and hydroxides. Fenitization and hydroxidation processes indicate that fluid saturation occurred during magma cooling of unit 4 and exsolved fluids which escaped through the unit 3 country rocks.

From the contact, inward textural variations include a hypersolvus alkali-feldspar quartz syenite, with less than 20% quartz in volume; a hypersolvus alkali-feldspar granite, with about 25% quartz; and a hypersolvus alkali-feldspar granite, with a radioactive accessory mineralogy. Widespread pegmatitic pockets are filled with quartz and alkali feldspar. Molybdenite platelets occurs within hydraulic breccias, with a matrix composed of quartz + calcite ± aragonite + hematite ± lepidocrocite.

At the inner contact below unit 4, a hypersolvus alkali-feldspar quartz syenite is exposed, which is likely to correspond to a foundered part of the unit 3 ring dyke.

A seven-point whole-rock Rb–Sr alignment has been obtained, including samples from the quartz-syenite–granite association of unit 4 and from the lower quartz syenite. The composite isochron yields a well-defined age of 7.9 ± 0.2 Ma, substantiating the complete thermal reset of the lower quartz syenite and a short 0.7-Ma period of quiescence between the emplacement of units 3 and 4. The unit 4 marginal facies yields a lower K–Ar age of 7.3 ± 0.2 Ma, which is likely to reflect thermal reset. A similar K–Ar age of 7.4 ± 0.2 Ma is given by a dolerite dyke intruding the unit 4 ring dyke.

Plutonic arcuate dykes Four incomplete ring dykes, 4–7 km in length, emplaced at, or near, the contact between units 2 and 3, are elongated along 45° to 80° arcs of circle and referred to hereafter as arcuate dykes. Their 150–300 m thickness has the same order of magnitude as the ring dykes that they intrude. The chief rock type is a porphyritic hypersolvus microsyenite. The first set of dykes, grossly coeval with unit 3, includes a 4-km long, 200-m thick arcuate dyke, with enclaves of unit 2 syenite and forming a breccia at the contact with unit 3 syenite, and another 7-km long 300-m thick arcuate dyke, emplaced within unit 2, crowded with 30% mafic enclaves forming a monzogabbro–monzodiorite–monzonite suite, that could represent dismembered cone sheets. The second set post-dates unit 3 with a 6-km long 150-m thick arcuate vertical dyke, with enclaves of unit 3 syenite, and another 5-km long 150-m thick arcuate dyke, with 10-cm wide enclaves of units 2 and 3 syenites, whereas aegirine dykelets cross-cut the wallrocks and the dyke itself.

Satellite cupolas The eastern part of the boundary fault of the southern ring complex is occupied by a bimodal population of cupolas. The first population comprises four small cupolas, with an average diameter of 300–400 m, whereas the second has a diameter of 3.0–3.5 km. Both basalt wallrocks and unit 1 quartz syenite were intruded, with subvertical contacts at the walls changing in a short distance into a horizontal contact at the roof. Brecciated screens of basalt emphasize the contact between the cupolas and the outer unit 1 ring dyke (Fig. 6). The K–Ar age of 9.1 ± 0.4 Ma on the Anse Syénite whole rock is consistent with field evidence that the cupola intrudes the *c.* 12-Ma unit 1. It is identical to the K–Ar age of 9.2 ± 0.4 Ma age obtained on an aplitic dyke cutting the alkali-feldspar quartz syenite of unit 2. The Anse Syénite cupola could therefore be younger than the unit 2 ring dyke and older than the unit 3 ring dyke. No age determinations are available so far for the other cupolas.

The northern ring complex

The northern part of Rallier-du-Baty igneous complex was *terra incognita* before the 1960s. The glacial-carved landscape is dominated by a central ridge of snow-covered or ice-capped summits, with elevations above sea-level varying between 1202 m (Dôme Carva) and 730 m (Table de l'Institut). Deeply dissected valleys, in which torrential rivers are flowing eastwards, westwards, or southwards, show characteristic glacial U- and V-shapes. The west coast is barely accessible by sea, but can be reached from the east by 500-m high passes open through the central ridge. Slopes are covered with scree and valley bottoms are filled with glaciofluvial gravel, whereas cliffs and river banks display reasonably fresh exposures.

Preliminary surveys during the 1974–1976 summer expeditions suggested four nested intrusive centres I, W, NE and N (Fig. 3), comprising no less than 17 different rock types and units (Giret *et al.* 1980; Lameyre *et al.* 1981), although K–Ar ages suggest only a 1.3 ± 0.4 Ma-long period of intrusion (Lameyre *et al.* 1976). Field evidence was carefully re-examined during

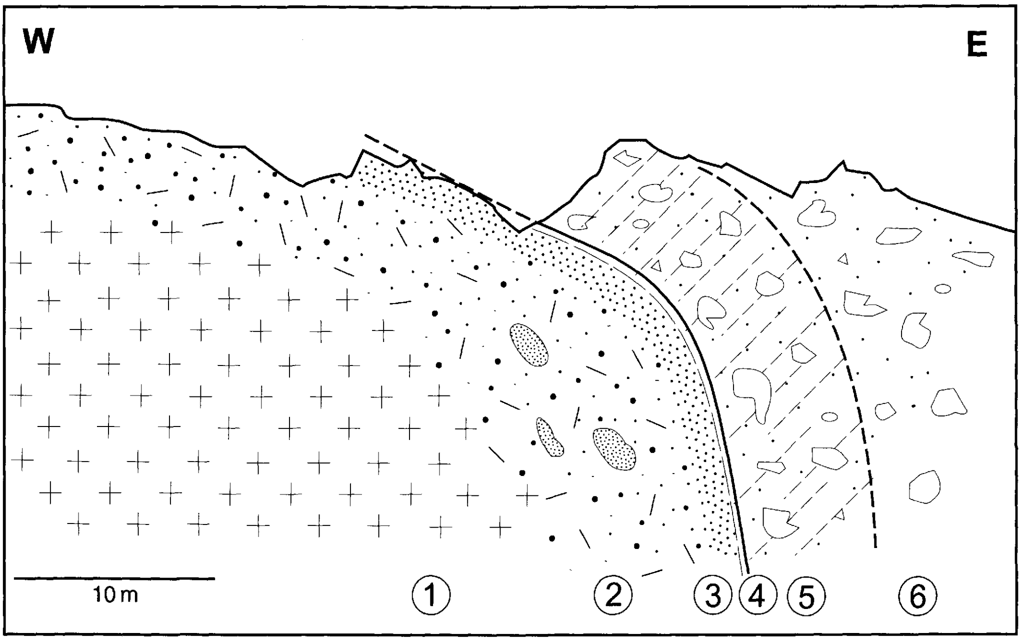

Fig. 7. Cross-section at the contact between Joliot–Curie caldera deposits with unit 6 syenite of the northern ring complex, as observed on the left side of Vallée des Contacts: 1, porphyritic coarse-grained zone; 2, medium-grained zone, with felsic fine-grained enclaves; 3, fine-grained zone; 4, finely fractured zone at the contact; 5, hornfelsed pyroclastic breccia; 6, pyroclastic breccia (sketch by Bonin 1995, unpublished).

the CARTOKER 94–95 summer campaign and critical interpretation of the observations resulted into the identification of only one single ring complex (Fig. 4), slightly larger in size than the southern structure, with a 18-km long N–S major axis and a 16-km long east–west minor axis. Seven discrete ring dykes and cone sheets, which intruded a dissected early caldera, were cut by two later (caldera) volcanoes.

Pre-plutonic caldera-filling volcanic formations: the Joliot-Curie caldera A 10 km × 1.5 km raft of trachyte pyroclastites was discovered in the northernmost part of the igneous complex, where it occupies the highest drainage basins of the rivers. It is bordered to the north by flood basalts and to the south by quartz syenite. The observed caldera-filling series comprises:

1 a poorly stratified lower sequence of pumice breccias, and
2 an upper sequence of pyroclastic flows with typical ignimbrite features.

The base and the total thickness of the series could not be observed. Intrusive, often autoclastic, domes and related feeder dykes are composed of porphyritic trachyte, which can be highly vesiculated.

The outer contact with the older horizontal flood basalts of the upper sequence consists of a vertical ring fault, culminating at Pic Joliot-Curie (1005 m above sea-level) and often hidden by scree and glaciers. The western segment of the border fault is marked by a double alignment of intrusive domes fed by dykes. The inner contact is outward dipping and displays, from the intrusive centre to the pyroclastites, the unit 6 coarse-grained porphyritic alkali feldspar quartz syenite passing to a 10-m thick medium-grained zone, with felsic fine-grained enclaves, to a 2-m thick fine-grained zone, to a 10-cm thick finely fractured zone at the contact, whereas pyroclastic breccias, converted into hornfels in a 5-m thick zone, are intruded by trachyte intrusions (Fig. 7).

Plutonic ring dykes and cone sheets Intrusive units were emplaced as either cupolas and ring dykes, or cone sheets. From the reappraisal of field evidence, they are numbered hereafter from 1 to 7, according to their order of decreasing age from the oldest to the youngest (Table 1).

1 The poorly represented hypersolvus alkali-feldspar syenite unit 1 covers a very small area on a 500-m high hill at the eastern side of the

Table 1. *The revised chronological sequence of igneous rocks: Rallier-du-Baty nested ring complex*

Geological units and formations	Emplacement age	Method	Reset age	Remarks	Reference
Pic Saint-Allouarn volcano	Post-Wurm to the seventeenth century	Field evidence			1
Dôme Carva volcano	Post-Wurm before	Field evidence		Radiometric dating currently in progress	5
Late ignimbrite and pumiceous falls	the seventeenth century				
Table-de-l'Institut caldera volcano				Radiometric dating currently in progress	
Trachyte pyroclastic flow in Vallée des Sables	1.15 ± 0.05 Ma	WR K–Ar			2
Northern ring complex					
Quartz trachyte unit 7	4.9 ± 0.02 Ma	WR K–Ar			2
Trans-solvus alkali-feldspar quartz syenite unit 6					
Hypersolvus alkali-feldspar quartz syenite unit 5		K-feldspar K–Ar	4.9 ± 0.2 Ma	Sample close to quartz trachyte unit 7	
	6.2 ± 0.2 Ma	WR K–Ar		Date not consistent with field evidence	
Hypersolvus alkali-feldspar quartz syenite unit 4					
Hypersolvus alkali-feldspar syenite–gabbro unit 3	5.6 ± 0.2 Ma	K–Ar on gabbro			
	5.7 ± 0.2 Ma	K–Ar on syenite			
Hypersolvus alkali-feldspar granite unit 2					
Hypersolvus alkali-feldspar syenite unit 1					
Joliot–Curie caldera volcano	> 6.2 Ma	Field evidence			5
Southern ring complex					
Dolerite dyke cutting unit 4	7.4 ± 0.2 Ma	WR K–Ar			2
Hypersolvus alkali-feldspar quartz syenite–granite unit 4		WR K–Ar	7.3 ± 0.2 Ma	Marginal facies close to a dolerite dyke:	
floored by hypersolvus alkali-feldspar quartz syenite				thermal reset or fenitization effect ?	
(foundered units 3 and 2?)	7.9 ± 0.2 Ma	WR Rb–Sr			
Hypersolvus alkali-feldspar quartz-syenite unit 3	8.6 ± 0.1 Ma	WR Rb–Sr			
Satellite cupola:					
Anse Syénite hypersolvus alkali-feldspar quartz syenite	9.1 ± 0.4 Ma	WR K-Ar			
Aplitic dyke cutting unit 2	9.2 ± 0.4 Ma	WR K–Ar			
Hypersolvus alkali-feldspar quartz-syenite unit 2	9.7 ± 0.2 Ma	WR Rb–Sr			
Hypersolvus alkali-feldspar quartz-syenite unit 1	*c.* 12 Ma	WR Rb–Sr			
	12.6 ± 0.4 Ma	WR K–Ar			
Early composite intrusion:		Biotite K–Ar	13.6 ± 0.4 Ma	Reset or cooling age?	
Anse du Gros Ventre gabbro	15.4 ± 0.5 Ma	WR K–Ar			
Flood basalt basement		WR K–Ar	11.5 ± 0.2 Ma	Thermal effects at 30 m from the contact with unit 1 of the southern ring complex	1
		Field evidence	15–12 Ma	Zeolitization event in the archipelago	3
	24–20 Ma	WR K–Ar		Feeder dykes of flood-basalt basement of the nearby (40 km) Mont Ross volcano	4

(1) Nougier (1970), (2) Dosso *et al.* (1979), (3) Giret *et al.* (1992), (4) Weis *et al.* (1998), (5) Gagnevin *et al.* (2003).

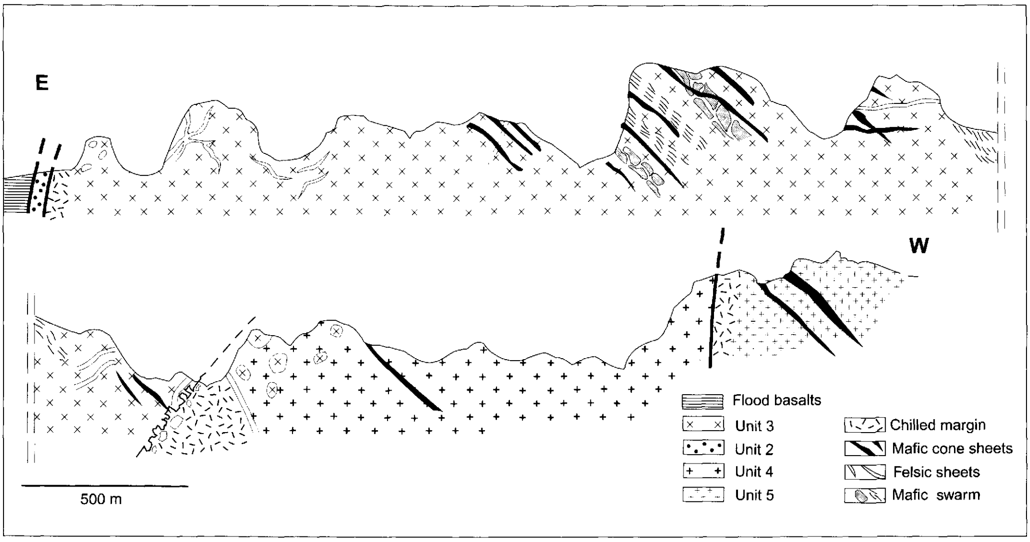

Fig. 8. General cross-section of the Vallée Milady, displaying the relationships between the different intrusive units and with the bimodal network of cone sheets and enclave swarms in the northern ring complex.

ring complex. The outer contact with basaltic wallrocks is marked by a chilled margin in syenite, whereas basalt was converted into amphibole hornfels.

2 The hypersolvus alkali-feldspar granite unit 2, sparsely exposed along the eastern contact, is observed on a hill where it intrudes unit 1, and on a 500-m long, 100-m high whaleback hummock on the left bank of Vallée Milady, where it intrudes basaltic wallrocks (Fig. 10). The outer contact with basaltic wallrocks is marked by quartz-rich pegmatitic and aplitic streaks within quartz-poor (20–25% in volume) granite. From the contact outwards, the recrystallized basalt shows a 1-m wide zone affected by magmatic stoping marked by a network of aplitic dykes, and a 10-m wide zone where columnar jointing was totally destroyed.

3 The composite hypersolvus alkali-feldspar syenite–gabbro unit 3 is one of the most important intrusions and covers a large area in the SE and western parts of the ring complex. The best exposure is located in Vallée Milady, where an almost continuous 2.5-km long horizontal cross-section is displayed (Fig. 10). From east to west, i.e. from outer (=top) to inner (=base) parts of the intrusion, the following facies variations were observed:

- a slightly porphyritic fine-grained marginal facies at the contact with unit 2;
- a porphyritic (0.5-cm long alkali-feldspar phenocrysts) fine- to medium-grained facies;
- a porphyritic (1-cm long alkali-feldspar phenocrysts) medium- to coarse-grained facies: the main facies. It is crowded by places with fine-grained felsic enclaves, interpreted as reworked pieces of chilled margin. Solidus to subsolidus volatile build-up is evidenced by fairly abundant pegmatitic lenses and veins, 5-cm thick amphibole schlieren resembling lindinosite (Lacroix 1922; Orcel 1924) and later millimetre-thick hydraulic breccias. Late 10–20 cm-thick dykelets are composed of alkali-feldspar syenitic aplite and granitic pegmatite.

The porphyritic medium- to coarse-grained main facies is dissected at less than 150 m away from the inner contact with unit 4, and forms 10-m to 1-m diameter angular or rounded stoped blocks set within a dense network of aplitic concentric dykes issued from the unit 4 alkali-feldspar syenite (Fig. 8).

The most striking feature of unit 3 ring intrusion is the supplementary occurrence of bimodal syenite–gabbro suites, emplaced as 0.5- to 10-m thick cone sheets into the solidifying syenite during at least three intrusive episodes (Fig. 8):

- the earliest suite constitutes an inward (westward)-dipping net-veined complex of miarolitic cavity-bearing alkali-feldspar syenite with coeval hybrid enclaves occurring in parallel streaks;
- the subsequent suite is characterized by a second inward-dipping net-veined complex

of fine-grained alkali-feldspar syenite and coeval mafic enclaves with cauliflower-shaped fractal contacts;

- the latest suite comprises a parallel set of inward-dipping 50-cm to 5-m thick felsic and mafic cone sheets, both with columnar jointing.

Net-veined complexes were preferentially emplaced into the porphyritic medium- to coarse-grained main facies, while cone sheets are developed within the marginal facies as well. Similar 5.7 ± 0.2 and 5.6 ± 0.2 Ma K–Ar ages on syenite and gabbro, respectively (Dosso *et al.* 1979, Table 1), agree with field evidence.

Elsewhere, a nearly vertical outer contact with recrystallized basaltic wallrocks is emphasized by aplitic syenite dyke swarms developed within a 200-m thick zone. Farther to the south, outward-steeply dipping sharp contacts with the intrusive units of the southern ring complex are exhibited, where the unit 3 syenite contains fine-grained enclaves, interpreted as dissected chilled margin, and miarolitic cavity-bearing xenoliths of quartz syenite and granite.

4 The hypersolvus alkali-feldspar quartz syenite unit 4 is one of the largest intrusions. It is exposed in the central and western parts of the ring complex, where it is in contact with basaltic country rocks. The outer contact with basaltic wallrocks, always marked by the finer-grained texture of unit 4 syenite, is nearly vertical at low elevation, outward-dipping and relatively flat, with intercalated basalt screens at higher elevations (about 250 m above sea-level).

Unit 4 comprises two unequally exposed facies. The less-represented facies is composed of coarse (5- to 7-mm long mesoperthitic alkali-feldspar crystals) even-grained alkali-feldspar quartz syenite, but the more extensive facies is a heterogeneous alkali-feldspar quartz syenite, with a medium-grained groundmass enclosing 10-cm large pegmatitic lenses and miarolitic cavities, providing evidence of magma volatile oversaturation. Miarolitic cavities, arranged in a network defined by 30-cm wide intervals, are infilled with alkali feldspar, quartz, fluorite and other minerals. Hydraulic breccias are represented by a 100-m wide cylindrical vent, infilled with a package of cemented syenite blocks, and by several smaller vents filled with silica minerals and sulphides (mainly pyrite), inducing stained and rusty aspect of the heterogeneous syenite.

Cone sheets are less numerous than within unit 3, and almost always composed of microsyenite. They yield sharp contacts and a symmetrical flowage structure derived from the Bagnold effect, with a vesicular core zone crowded with elongate 1-cm long alkali-feldspar phenocrysts, and aphanitic border zones with scarce globular 1- to 1.5-cm diameter alkali-feldspar phenocrysts. Cone sheets were emplaced later than hydraulic breccias.

Relationships with unit 5 are difficult to decipher, as most contacts are covered with scree. In a 10-m wide contact zone, unit 5 medium-grained syenite, containing decimetre-scale round enclaves of unit 4 heterogeneous syenite, develops metre-scale pillow-like rafts within unit 4 syenite. This observation suggests emplacement of unit 5 magma when the still-hot unit 4 was not yet consolidated and perhaps partly liquid.

5 The hypersolvus alkali-feldspar quartz-syenite unit 5 constitutes the most central part of the ring complex. The exposed areas were disconnected, due to subsequent emplacement of the Table de l'Institut caldera volcano. Salient features of unit 5 are abundant quartz (up to 15% in volume) and biotite as the chief mafic mineral component.

Unit 5 shows no contact relationships with basaltic country rocks. It is adjacent to unit 4, and the only exposed contact yields ambiguous features (see above). The unit 5 quartz syenite is intruded by the unit 6 quartz-syenite cupola, and the unit 7 quartz-trachyte dyke.

The K–Ar ages (Table 1), 6.2 ± 0.2 Ma on whole rock and 4.9 ± 0.2 Ma on alkali feldspar, should be reassessed. The 'old' 6.2-Ma age does not agree with field observations that unit 5 quartz syenite is younger than the 5.6–5.7-Ma unit 3 gabbro-syenite. The 'young' 4.9-Ma age was likely to be reset during emplacement of the later unit 7 quartz-trachyte dyke.

Units 4 and 5 syenites are cross-cut by a 1-km wide quartz-poor hypersolvus alkali-feldspar granite stock, which, accordingly, constitutes a post-5 unit. No contact relationships with units 6 and 7 are displayed in the field, so that no more precise chronology of the stock can be ascertained.

6 The porphyritic trans-solvus alkali-feldspar quartz-syenite unit 6 occupies the NE and northernmost parts of the ring complex. The salient feature of unit 6 syenite is the trans-solvus alkali-feldspar assemblage (Bonin 1972; Martin & Bonin 1976), with euhedral mesoperthite crystals set within a groundmass composed of quartz, K-feldspar, and albite graphic intergrowths. At the contact with wallrocks, recrystallized basalt of the lower

sequence hosts a network of aplitic syenite dykes, and unit 6 syenite encloses large basalt screens. Inwards, textural variations within unit 6 syenite include: a chilled margin with acicular alkali feldspar, a fine-grained facies crowded with 0.5–1-cm diameter miarolitic cavities set at 5- to 10-cm wide intervals, a medium-grained facies, and a coarse-grained facies with scarce fine-grained enclaves.

Contact relationships with Joliot–Curie caldera-filling pumice breccias and trachyte domes and with unit 5 quartz syenite confirm that quartz-syenite unit 6 is younger.

7 The quartz trachyte unit 7 is made up of a SE-dipping SW–NE trending, 50- to 200-m thick dyke. The quartz trachyte has rhomb-shaped millimetre-long alkali-feldspar phenocrysts set within a fine-grained to microcrystalline groundmass, and contains devitrification spherulites. It intrudes unit 6 quartz syenite and unit 5 quartz syenite. The K–Ar age of 4.9 ± 0.2 Ma (Table 1) agrees with field evidence, as does the identical alkali-feldspar K–Ar reset age determined on a unit 5 sample collected near the quartz-trachyte dyke.

Later volcanoes

Volcanic formations intrude and/or overlie the Late Miocene plutonic ring dykes and cone sheets in the central and southern parts of the northern ring complex. Two discrete calderas were identified, which document a renewed magmatic activity. The first 10-km diameter caldera is centred on the 730-m high Table de l'Institut. The second 8-km diameter volcano is barely exposed as nunataks under glaciers and centred on the 1202-m high ice-covered Dôme Carva. Pyroclastic and lava flows filled up caldera craters and flowed down outside, along glaciofluvial valleys. Huge amounts of associated air falls were deposited throughout the Kerguelen archipelago.

The Table de l'Institut caldera volcano The Table de l'Institut caldera volcano was discovered by Marot & Zimine (1976). The K–Ar age of 1.15 ± 0.05 Ma (Dosso *et al.* 1979) obtained on an extra-caldera trachyte pyroclastic flow document an apparent 3.75 ± 0.25-Ma long period of magmatic rest. Caldera-related formations occupy a large area within and outside the border ring fault (Gagnevin *et al.* 2003). They are subdivided into:

1 caldera-filling formations,
2 late- to post-caldera trachytic formations, and
3 late- to post-caldera basic to intermediate formations, which were erupted in that order during build-up and subsequent destruction of the volcano.

The border ring fault is frequently hidden by late pyroclastic flows in the valleys and by scree on the summits, but it is marked locally by a 10-m thick porphyritic trachyte ring dyke. Along the near-vertical ring fault, contacts are sharp with older units 4 to 6 alkali-feldspar quartz syenites. In the vicinity of the fault, volcanic formations were tilted, with an inward dip up to 45°, and are cross-cut by a swarm of aplitic dykelets and sills.

1 The caldera-filling formations are composed of pyroclastic flows and falls, lava flows are comparatively rare, and no intercalated epiclastic deposits were identified. Field survey documents a *c.* 600-m thick volcaniclastic pile constituted by three stratigraphic units. As the bottom of the caldera is nowhere exposed, the lowest part of the pyroclastic units remains unknown.

The lower pyroclastic unit was observed on a thickness of 100–120 m. It is composed of conformable coarse layers of trachytic breccia containing angular blocks (5–20 cm) of syenite. Two superimposed series were observed:
(i) a *c.* 20-m thick green lower series and
(ii) a 80–100-m thick black upper series.

The 400–500-m thick upper pyroclastic unit is dominated by barely layered and poorly sorted pumice agglomerates, breccias and tuffs. The sizes of the pumice fragments range from 2 cm to 2 m. Pumice tuffs turn locally into true ignimbrites showing up to 20-cm long and 2-mm thick fiammé, implying high-temperature deposition and welding.

The uppermost Table-de-l'Institut unit is restricted to the top of the 730-m high summit. It is made up of 1-km wide and 50-m thick massive unit of porphyritic trachyte, conformably overlying the upper unit. The horizontal basal contact is completely hidden by scree composed of large boulders of trachyte. The massive lava-like rock is composed of a groundmass, speckled with phenocrysts of anorthoclase–sanidine and rare mafic minerals. This late unit is interpreted tentatively as the result of cooling of an ultimate lava lake at the very end of the syn-caldera volcanic episode.

Mafic rocks occur as hypabyssal units, that could be related for the most part to late- to post-caldera volcanic episodes. The only exception is represented by rare and small (50-m long and 3-m thick) hawaiite–mugearite vesicular lava flows, intercalated within the pumice tuffs of the low part of the upper pyroclastic unit, implying they were erupted during the syn-caldera volcanic episode. Dykes and sills, some of which are related in the form of 'jumping sills', were observed throughout the caldera-filling volcaniclastic pile. Their thicknesses range from 1 to 5 m and they consist of hawaiite–mugearite.

2 The late- to post-caldera trachytic formations are chiefly composed of welded pyroclastic flows. They partly infill the bottom of large U-shaped valleys created by glacial erosion of the volcano. The K–Ar age of 1.15 ± 0.05 Ma was obtained in one of these flows. The flows are arranged as a network radiating from and originating in the central part of the caldera. They are interpreted as the result of late- to post-caldera explosive eruptions occurring during and/or after destruction of the original topography. The eruptive vent could be located in the unexposed icy area south of Table-de-l'Institut.

Trachyte pyroclastic flows are several kilometres long and 30–50-m thick. The most impressive pile inside the caldera displays five discrete superimposed pyroclastic flows, each 50-m thick. They constitute a 250-m high riegel which determined upstream a flat basin, now filled in with volcaniclastic gravel and sand lacustrine deposits, with just a residual lake located in its NW tip. Pyroclastic features, such as up to 30-cm long and 3-cm wide glass shards, and up to 1–2-m diameter blocks of syenite and trachyte set up within a porphyritic groundmass, provide evidence of turbulent to chaotic flow and high-temperature welding. During consolidation, pyroclastic flows developed conspicuous columnar jointing, with the diameters of the prisms about 0.5 m in the upper half, and 1 m in the lower half.

Pyroclastic flows rest generally upon the within-caldera upper pyroclastic unit and units 4 to 6 alkali-feldspar quartz syenites. They overlie seldom alluvial deposits and pumice tuff deposits. Pumice tuff deposits are barely layered at all, and are poorly sorted – also implying turbulent flow, but at lower temperature. Their thicknesses are various and can reach up to 150 m. From stratigraphic evidence, pumice tuff deposits are interpreted as resulting from incipient explosive eruptions, that subsequently emitted the associated pyroclastic flow.

3 The late- to post-caldera mafic units are made up of two discrete rock types, issued from eruptions of contrasting styles: hawaiite, speckled with plagioclase phenocrysts and largely exposed in the NE valleys, and mugearite, bearing ternary feldspar phenocrysts and restricted to the Vallée du Telluromètre.

Within the caldera, and along the border ring fault, hydromagmatic eruptions created maars, and emitted surges and lava flows. Four 0.4- to 1.5-km-diameter maars were identified in the plateau below and to the SE of Table-de-l'Institut. Although eroded, the maar structure is grossly preserved, with a flat-dipping outer tuff-ring and a steeply dipping inner tuff-ring. The nearby basement yields impact figures caused by the ballistic fall of large blocks. From bottom to top, tuff-rings are made up of a 5–10-m thick lower unit of breccia to cinerite, with blocks of basement rocks showing no evidence of fresh magma, and an up to 150-m thick upper unit, characterized by cauliflower-shaped mafic bombs and/or soaked vitreous lapilli set within a palagonitic matrix, providing evidence of the incorporation of fresh magma into a wet environment. The upper unit is intruded by rheomorphic breccia dykes. The individual layers display dune and anti-dune structures, along with highly variable grain sizes and centimetre- to decimetre-scale thicknesses.

Outer tuff-rings are so well developed that they can constitute a nearly uniform blanket on the plateau below the Table-de-l'Institut. A basal unit of breccia containing vitreous lapilli is overlain by an upper unit of breccia with angular blocks of basement rocks (syenite, trachyte) and of bombs of hawaiite, providing evidence of transition from hydromagmatic to strombolian dry magmatic styles of eruption. Downstream, this sequence of eruptive events is illustrated by basal surges capped by 5–15-m thick block (aa) lava flows.

Other hawaiite lava flows issued from cinder cones located outside the caldera. In the Vallée des Chicanes, a highly eroded 1-km large cinder cone constitutes a small riegel on the right bank of the river. It was built by strombolian-type eruptions, that jetted a 100-m thick blanket of bombs and blocks, filling a former valley, and overlain by three superimposed 5–10-m thick hawaiite block-lava flows, with 0.5–1-m-scale columnar jointing. Upstream, a supplementary hawaiite block-lava flow was emitted from a small vent related to a mafic dyke, and overlies a 20–30-m thick spatter of vesiculated bomb fragments.

Mugearite is exposed in the flat area located in the south of the deltaic mouth of the Vallée du Telluromètre. It constitutes a 10–20-m thick lava

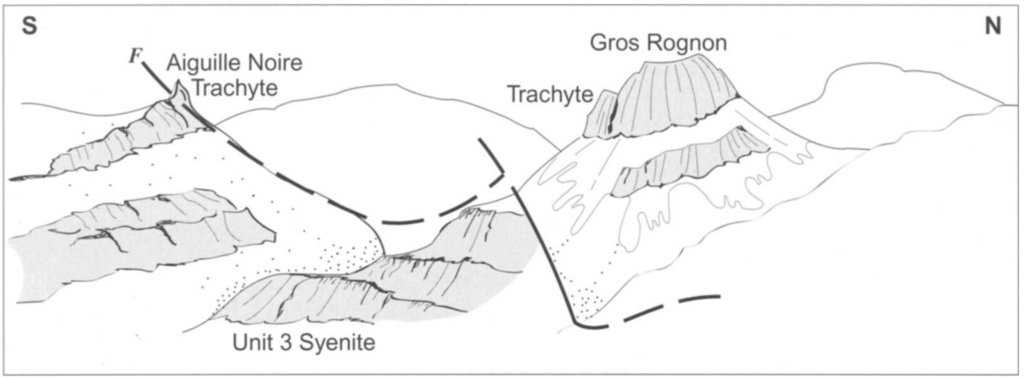

Fig. 9. Sketch of the cliffs above Vallée de Larmor (Bonin 1995, unpublished). The border fault of the Dôme Carva volcano is marked by trachytic pyroclastic flows inside and unit 3 syenite of the northern ring complex outside. The summits in the background are fully covered by ice and snow.

flow filling a former large valley. The related vent was not identified; it is probably hidden by later volcanic formations upstream. The lava flow rests directly upon unit 3 and 4 alkali-feldspar quartz syenites and, locally, alluvial deposits, with no intercalated spatters, and is overlain by pyroclastic formations issued from the Dôme Carva volcano. Columnar jointing is well developed. Steam that issued from the boiling of water contained in the alluvial deposits excavated a hydrothermal chimney through the lower part of lava flow and created a cave used by seal hunters.

Dôme Carva volcano The Dôme Carva volcano was identified during the CARTOKER 94–95 summer expedition. At elevations above sea-level higher than 600 m, the topography is entirely dominated by a 50-km^2 ice-sheet culminating at 1202 m near Dôme Carva, with the exception of scarce nunataks: most of them, but not all, being located close to the border fault (Fig. 9). Glacier tongues radiate from the ice sheet and flow downwards. However, their lengths were strongly reduced during the last 30 years, so that they can no longer reach the seashore and only partly fill the glacial valleys that they created or enlarged.

The border fault could not be observed in the field, because it is hidden by scree and ice. It is marked by sharp cliffs composed of trachyte flows. The trachyte volcanic products comprise volcano-filling and late to post-caldera units, erupted during build-up and subsequent destruction of the volcano. No radiometric dates are available so far.

1 Volcano-filling formations are almost completely capped by the ice sheet, except in the periphery of the volcanic complex. Their total thickness is about 300 m – approximately half of that of Table-de-l'Institut caldera formations. The following stratigraphic sequence, exposed in valleys and banks of glaciers, displays, from bottom to top:
   - alkali-feldspar quartz-syenite unit 4, constituting the basement;
   - three 50-m thick trachyte pyroclastic flows developing 5–10-cm thick lamination and 1–2-m-scale columnar jointing, and yielding the (biotite + sanidine) phenocryst assemblage;
   - 100-m thick layered and poorly sorted breccia, with up to 20-cm diameter blocks of obsidian and pumice set within a palagonitic matrix. Enclaves of coarse-grained leuco- to mesocratic alkaline rocks were found as boulders at the exit of a small defile. With their conspicuous magmatic planar foliation, these rocks are likely to represent ejecta from a deep-seated magma chamber. No mantle nodules were found, which provides further evidence that deep-seated reservoirs stored this kind of enclave.
   - 100-m thick layered and better-sorted tuffs and breccia, with blocks of obsidian and pumice set within a vitreous matrix;
   - two superimposed 20–30-m thick trachytic units forming a plateau like the Table-de-l'Institut unit and tentatively interpreted as filling up a lava lake at the end of the volcanic episode;

2 Late- to post-caldera units are chiefly composed of trachyte pyroclastic flows. They fill the bottom of glacial valleys that were excavated partly through caldera-filling formations, partly outside the caldera.

- The first major event produced a series of 30–50-m thick pyroclastic flows, exposed close to the border ring fault and outside the caldera in the western coastal area. Pyroclastic flows rest directly upon their basement; intercalated pumice tuffs are scarce or lacking. Lava tubes and 5–10-cm thick lamination developed during flowage, followed by 1–2-m-scale columnar jointing during cooling. Porphyritic trachyte is characterized by sanidine phenocrysts up to 5 mm in size.

  The most complete sequence was observed in the Vallée du Telluromètre. A lower unit, formed by a package of small valley-filling linear pyroclastic flows resting upon alkali-feldspar quartz syenite of unit 4, constituted a riegel in the middle part of the valley, where it produced a naturally dammed lake, now filled with finely layered and well-sorted lacustrine silt deposits. It is overlain by an upper unit of large pyroclastic flows, forming a 100-m high cliff above the valley.

  In the western coastal area, the sea-shore is occupied by the lower unit filling the older glacial valleys and resting upon quartz alkali-feldspar syenite units 3 and 4 as well as upon mugearite lava flows of the Table-de-l'Institut caldera. The upper unit is composed of extensive sheets of pyroclastic flows capping a formerly flat area.
- The second major event was marked by a dramatic explosive eruption, that originated in a vent located to the east of Dôme Carva. Its presumably young age is argued by the following evidence: the related tephras, widespread in the Rallier-du-Baty Peninsula, cover all formations up to the Quaternary alluvial fans and are overlain only by the glacier tongues, that made their maximum extension during the Little Ice Age in the eighteenth century (Nougier 1970). Glacier-forming blue ice contains numerous thin ash layers, suggesting that ice was formed by snow compaction at least partly during ash eruptions. Two discrete types of tephra can be distinguished: ignimbritic flows v. ash and pumice falls.

  Ignimbritic flows are heterogeneously welded and were extensively removed by glaciofluvial erosion. They constitute 3–5-m high residual buttes scattered within the bottom of large valleys, or in saddle-like passes between major drainage basins. They are grossly arranged as a network radiating from the unexposed icy area between the La Pérouse and Arago glacier tongues, where the eruptive vent is inferred to be located. The best preserved 130-m thick ignimbritic flow, observed on the left side of the Vallée du Telluromètre, rests upon quartz alkali-feldspar syenite unit 4, forming a rounded butte, and on the lower trachytic unit of the first late- to post-caldera event, and displays from bottom to top:

  - a 50-m thick welded ignimbrite displaying occasional 2–5-cm thick lamination and constant 3–5-m large columnar jointing. Huge fiammé, which can reach up to some metres in length and up to 5–10 cm in width, are associated with large blocks of obsidian and vesiculated pumice set within a vitreous-grained matrix. Overall chaotic and welded texture, as well as poor sorting of matrix grains, suggest high-temperature turbulent flow, compaction, and welding.
  - 30-m thick unconsolidated tuffs and breccias, above a ledge used by albatrosses for nesting, corresponding to the transition from welded to unwelded materials. Overall chaotic texture and poor sorting of matrix grains suggest again turbulent flow, but unwelded characteristics imply lower-temperature compaction.
  - 50-m thick well-bedded and well-sorted ash and lapilli layers suggest air-fall deposition, with no evidence for turbulent flow. They are covered by blocks of sanidine-bearing ignimbritic obsidian and of floating pumice fragments.

  Unwelded ash and pumice falls cover large areas on the whole of the Rallier-du-Baty Peninsula. Where these deposits were not protected by ignimbritic flows, they were removed and subsequently redeposited. Epiclastic alluvial fans comprise a number of 10–20-cm thick cross-bedded layers of 2–3-cm long pumice clast-bearing coarse-grained sandstone, intercalated with 10-cm thick well-bedded layers of finer-grained sandstone, carrying crystal lapilli and 1–3-mm long pumice clasts. Contrasting styles of deposition: glaciofluvial lenticular bedding alternating with aeolian well-sorted sand blanketing, resulted from discrete periodic episodes related to climatic changes. Low-relief areas are covered everywhere throughout the Kerguelen Archipelago by reworked 2–3-cm long matrix-supported pumice clasts.

The Pic Saint-Allouarn volcano The southern ring complex is dominated by high summits covered by a 400-m thick ice sheet extending continuously from Dôme Carva to Pic Saint-Allouarn (1189 m above sea-level). Trachyte pyroclastic flows, emerging from below the ice and probably aided by melting of the ice sheet, diverge radially from a centre located at Pic Saint-Allouarn. The present state of the vegetation on the Grande Coulée and the Wurmian glacial deposits overlain by the Coulée de Vulcain indicates that the eruptions have occurred very recently and could have been as late as during the Little Ice Age of the eighteenth century (Nougier 1970).

Thermal activity

Fumaroles were discovered by seal hunters. Six fumarolic fields are known in the Rallier-du-Baty Peninsula, covering a 50-km^2 area centred on Pic Saint-Allouarn: five on its western side and one on its eastern side. Each field comprises at least 10 vents, each with a diameter of about 10 m. The temperature at the vents ranges from 30 to 105 °C and the pH from 3.9 to 9.5. The geothermal source could correspond to a 2-km deep cooling trachytic body (Verdier 1989). Limited activity is shown by the temperature of the hydrothermal fluids being estimated at less than 350 °C, very low contents of reduced carbon and hydrogen species, and scarce hydrothermal deposits (sulphur, pyrite and hematite). The northern fields lack sulphide deposits and yield five times lower radon abundances than the southern fields, indicating that they are less active (Delorme *et al.* 1994).

Evidence for current thermal activity elsewhere in the archipelago is rather meagre, with mild (18–20 °C) to hot (63 °C) thermal springs in the Central Plateau, and low-temperature carbonated springs west of the Mont Ross volcano (Verdier 1989).

Time durations and dimensions: implications for growth mechanisms

Erosion has removed most of the caldera volcano-filling formations, which are preserved only along the northern rim of the massif. Below the volcanic cover, a large volume of plutonic rocks was also scavenged by glaciers during the Quaternary ice ages. Thus, the volumes of magmas involved during the last 15 Ma in the build-up of the nested ring complex cannot be evaluated accurately. Only rough estimations will be provided.

Age relationships

The stratigraphic–geochronological chart of the Rallier-du-Baty Peninsula (Table 1) shows that the 15 Ma-long set of igneous episodes, starting with the early composite intrusions and persisting with the latest volcanic manifestations, encompasses the Late Neogene activity in the archipelago:

- The 15.4–12.6-Ma plutonic events, represented by the early composite intrusions and the unit 1 ring dyke of the southern ring complex, yield the same ages as the 16.6–12.4 Ma Ile de l'Ouest complex, the 13.7-Ma Société de Géographie pluton and the late 12.6-Ma trachyte dykes of Monts Ballons. They post-date the faintly zeolitized 17-Ma Monts Ballons and Iles Nuageuses complexes (Giret 1990) and are roughly coeval with the extensive zeolitization event affecting the older flood basalts (Giret *et al.* 1992). All the coeval complexes are located in the western part of the archipelago and yield silica-oversaturated to slightly undersaturated compositions.
- The 9.7–7.4-Ma plutonic events, represented by the other ring dykes and related cone sheets and dykes of the southern ring complex, are coeval with the 10.2–6.6-Ma tephrite–phonolite, strongly silica-undersaturated suite of Ronarc'h and Jeanne d'Arc Peninsulas, located in the SE part of the archipelago (Leyrit 1992).
- By contrast, the 6.2–4.9-Ma plutonic events of the northern ring complex seem to have no igneous counterparts in the rest of the archipelago.
- The 1.15-Ma to recent volcanic activity, manifested by the eruptions from the Table-de-l'Institut, Dôme Carva and Pic Saint-Allouarn (caldera) volcanoes, is tightly coeval with the 1.02–0.13-Ma slightly silica-undersaturated Mont Ross volcano, located 40 km east of the Rallier-du-Baty Peninsula (Weis *et al.* 1998). However, the activity on the Rallier-du-Baty Peninsula has persisted well after the extinction of the Mont Ross volcano.

The duration of the igneous activity within each complex decreases drastically with time. The discrete episodes which built the southern ring complex are defined within a 8-Ma period of time. The northern ring complex was emplaced during only 1.3 Ma. The Quaternary (caldera) volcanoes were active during about, or less than, 1 Ma. Now is apparently a period of quiescence, but the persistent fumarolic fields show that the igneous activity should not be considered as definitively extinct.

Dimensions and volumes

The two plutonic ring complexes have similar sizes: 17 km (east–west) × 15 km (north–south) for the southern centre, versus 18 km (north–south) × 16 km (east–west) for the northern one. Each plutonic complex is composed of discrete intrusive units, with a limited number of *c*. 1-km thick ring dykes and numerous 10-m thick cone sheets and arcuate dykes. According to field observations, each complex is about 2–4-km thick and the estimated volumes of plutonic rocks range from 400 to 800 km^3 in the southern centre, and from 450 to 900 km^3 in the northern one.

Although the coeval volcanic rocks emitted from the now-eroded overlying calderas have almost completely disappeared, their volumes could be of the same order of magnitude, ignoring the huge volumes of volatiles released. The southern ring complex would then correspond to 800–1600 km^3 of magmas and the northern one to 900–1800 km^3. As it took 8 Ma for the build-up of the southern centre, and only less than 1.5 Ma for the northern one, the average rates of magma supply differed by an order of magnitude: 0.003–0.004 $m^3 s^{-1}$ and 0.02–0.04 $m^3 s^{-1}$, respectively.

With the mean diameter of the Table-de-l'Institut caldera volcano being 8 km, the total volume of the 600-m thick caldera-filling trachytic formations is at least 30 km^3. This figure represents a minimum, because the base of the volcanic units was not observed. Hawaiite and mugearite products are comparatively more restricted in volume.

The Dôme Carva volcano has a mean diameter of 5 km; the total volume of the 300-m thick volcano-filling formations is about 6 km^3. The volume of the 80-m thick ignimbritic flows, which are accompanied by ash air-fall deposits blanketing the whole Kerguelen Archipelago, is estimated at *c*. 1 km^3. Several cubic kilometres of products jetted during this single eruptive episode can be envisaged, suggesting that the whole archipelago could have been covered by an up to 1-m thick blanket of pumice clasts driven from the vent by westerly winds. This explosive event was certainly one of the most powerful eruptions in the recent times in the Kerguelen Archipelago.

In the Yellowstone volcanic system, which yielded sizes of the same order of magnitude as the Rallier-du-Baty nested ring complex, it is assumed that 67 to 75% of the volumes of volcanic products were ejected in the atmosphere and lost during the explosive eruptions (Christiansen & Blanck 1972). If this was the case in the Rallier-du-Baty Peninsula, the Table-de-l'Institut caldera volcano could have erupted a volume of trachyte of about 90–120 km^3, and a total volume of 100–150 km^3. Although no plutonic equivalents have been identified so far, their volumes could be of the same order of magnitude. For the same reasons, the erupted volume of about 6–7 km^3 in the Dôme Carva volcano and the southernmost centres could reflect a more likely figure of 25–30 km^3.

Considering the volcanic formations coeval with the plutonic centres, but now vanished; the volcanic projections lost in the atmosphere; and the plutonic rocks coeval with the caldera volcanoes, but not yet exposed, the total volume of magmatic products emitted over 15 Ma could be estimated roughly at 2800 ± 850 km^3. Large volumes of magmatic products were removed early during the eruptions and later on by erosion, so that the Rallier-du-Baty Peninsula is occupied now by 1450 ± 450 km^3 of new materials, either exposed, or hidden – added to the Kerguelen crust. Their average thickness of 3.5 ± 1.0 km implies a crustal growth of 100 000 ± 30 000 m^3 per year (*c*. 0.003 ± 0.001 $m^3 s^{-1}$).

These values should be considered as minimum numbers. Cumulative xenoliths occur in volcanic breccias, indicating that mafic and intermediate magmas were emplaced within the lower crust, where by various differentiation processes they generated the highly evolved silicic magmas of the Rallier-du-Baty nested ring complex (Gagnevin *et al.* 2003). So far, their volumes have not been assessed precisely. Seismological studies indicate a 15–20-km thick crust beneath the nearby Mont Ross volcano (Recq *et al.* 1994). It is speculated that the Kerguelen Archipelago and even the surrounding plateau (Charvis *et al.* 1995) represent a continental nucleation process (Grégoire *et al.* 1998).

Growth mechanisms

The Rallier-du-Baty nested ring complex is dominated essentially by large ring intrusions, composed on top by a shallow 500-m to 1-km thick subhorizontal sheet and, at depths, by a vertical to steeply outward-dipping 50-m wide ring dyke. The upper sheet is occupied by a volume of magma of 100–200 km^3, whereas the ring dyke, with a 16-km diameter and an assumed 10–15 km vertical height, has a volume of only 12–18 km^3. As for all plutons, there is a 'room problem' to solve. Because neither flowage, nor melting of wallrocks, have been observed, the silicic magmas were likely to have been emplaced in a brittle fashion. The classical mechanisms of emplacement that have been identified so far in a brittle environment include: roof lifting, stoping and floor subsidence.

Tilting and doming of the basaltic wallrocks

Radial tilting of the flood basalts, centred on the Rallier-du-Baty Peninsula, is observed up to 20 km away (Fig. 10). Near the contacts with the

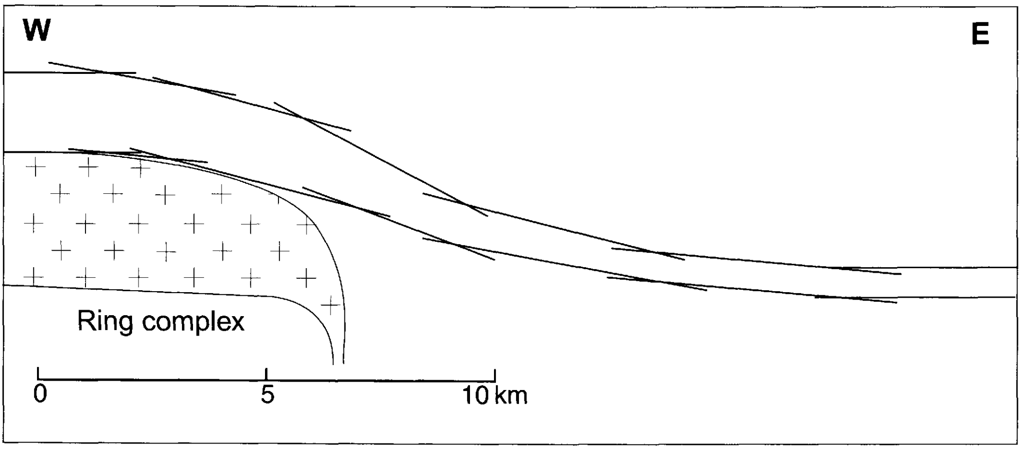

Fig. 10. Uplift and tilting of Neogene flood basalts above the Rallier-du-Baty ring complex, as deduced from the variation of measured dips of individual flows (after Marot & Zimine 1976).

ring complex, outward dips can reach 30°, and vertical uplift of the country rocks is estimated to range from 2.5 to 3.5 km (Nougier 1970; Marot & Zimine 1976), suggesting that roof lifting could be one of the major mechanisms of emplacement. However, two lines of evidence argue against a significant role played by roof lifting. The sidewall contacts with the country rocks are represented by a sharp unconformity, yielding an outward dip higher than that of the flood basalts. The *c.* 40-km diameter of this structural feature, approximately twice the 16-km mean diameter of the intrusions, cannot indicate a simple roof lifting mechanism, such as that advocated for laccoliths (Corry 1988). It is suggested that the structure could have originated by emplacement within the lower crust and progressive inflation of a dense network of magma chamber(s) (Grégoire *et al.* 1998). Such a network would be responsible for the protracted magmatic activity in the peninsula during the last 15 Ma.

Extent of stoping process The process of blocks of country rocks sinking from the roof of a pluton into a magma is described as 'stoping'. The principal line of evidence for the feasibility of such a process in the Rallier-du-Baty nested ring complex is the common occurrence of blocks of nearby wallrocks in almost all marginal facies of the plutonic intrusive units. The problem with the stoping mechanism is not whether it could act. It did, but at what scale? As noted by Clarke *et al.* (1998), a major question is: what proportion of the total ascent of a magma can stoping account for? Although producing spectacular exposures, stoping in the Rallier-du-Baty nested ring complex is always a process limited to a thickness of some tens of metres constituting the external marginal zones of the 500–1000-m thick ring intrusions. These field observations substantiate that stoping alone could not provide more than 5–10% of the space accommodated by the ascending magmas. However, the mechanism could play a role in the final shape of the intrusion and explain, e.g. the polygonal outline of the external contact of the alkali-feldspar syenite–granite unit 4 of the southern complex.

Cauldron subsidence Emplacement of a ring intrusion is basically governed by subterranean subsidence of a piece of brittle upper crust (Fig. 11). Space for the shallow intrusive sheet is provided along a flat tensile fracture opened through vertical translation of the sinking block moving downwards as a piston along a cylindrical boundary fault into the underlying magma chamber (Clough *et al.* 1909; Billings 1943). Although differing by an order of magnitude, a similar sequence of space-making processes, involving successively minor roof uplift and regional doming; floor subsidence by a major piston mechanism; and local stoping, favoured emplacement of the Coastal Batholith of Peru (Haederle & Atherton 2002).

An upper-crustal-scale balance in the rates of magma extraction from the chamber, magma ascent and intrusion-filling is required, while mass transfer from the chamber to the intrusion is accommodated by upper-crustal embrittlement. Magmas cooled and crystallized in a fairly static environment, as evidenced by weak

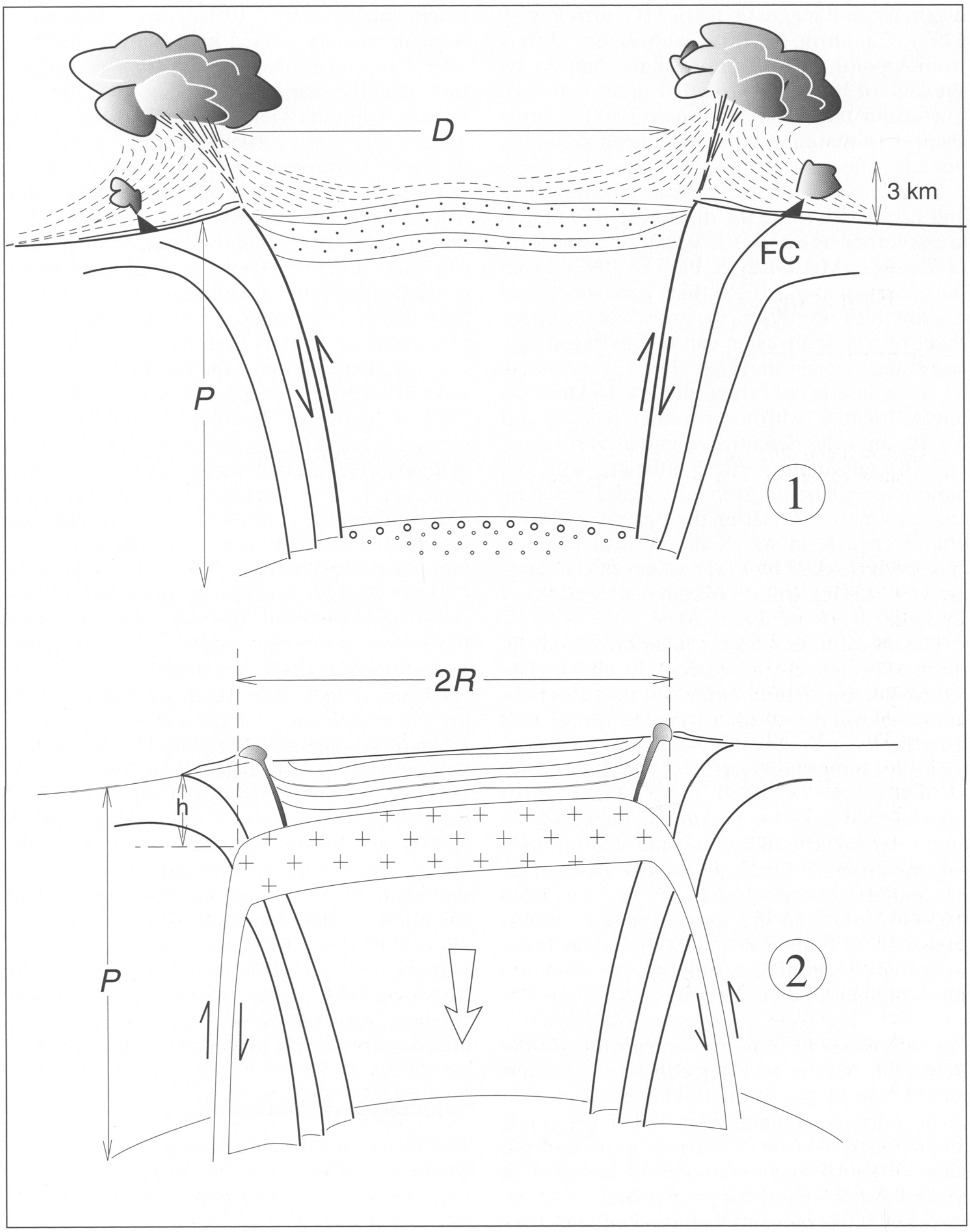

Fig. 11. Schematic cross-sections of an active caldera-related ring complex structure (adapted from Bonin 1986). The sequence of events 1 and 2 may be repeated several times before completion of the magmatic episode. $D = 2R$, diameter of the caldera; P, depth of the roof of the reservoir; h, depth of emplacement of the ring complex. (**1**) Magma overpressure, mostly due to exsolution of a vapour phase below the roof of a deep-seated reservoir, induces upward movement of the overlying crustal block (uplift can reach 3 km), initiation of inward-dipping reverse faults, explosive eruptions, deposition of pyroclastic formations (dots) within and outside the caldera, and emplacement of cone sheets and lateral sills (FC). (**2**) After the explosive eruptive event, a crustal block sinks into the reservoir, inducing outward-dipping normal faults, void space between caldera-filling volcanic formations and the subsiding block, and emplacement of a ring complex (crosses).

magmatic and magnetic fabrics (Geoffroy *et al.* 1997). Cauldron, or floor, subsidence differs from lopolith floor-depression mechanism by the lack of broadly distributed deformation of low strain magnitude (Cruden 1998). Simple shear deformation was, instead, localized on the boundary fault.

The dimensional parameters: T = thickness and L = length (here the diameter), of a pluton are governed by a power-law relation in the form of $T = bL^a$ (McCaffrey & Petford 1997). From the observation of *c.* 10-m thick cone sheets and *c.* 1-km thick ring dykes, the growth of the upper sheet of a ring intrusion can be envisaged as a two-stage mechanism (Figs 11 & 12) including: (i) self-affine propagation along a 16-km wide tensile fracture, with the parameters $a \approx 0$ and $b \approx 10$, until the definitive diameter is reached, and (ii) self-affine vertical inflation, with the parameter a tending to infinity and T reaching about 1 km. It differs from the current models of pluton growth, in which the vertical inflation episode is marked by lower values of the parameter a varying from 6 (Cruden & McCaffrey 2001) to 1.36 (Rocchi *et al.* 2004).

The time duration for the inflation episode by floor subsidence was extremely short. The Rb–Sr isotopic determinations of the successive intrusions of the southern centre reveal that these high Rb–Sr magmas could not remain isotopically homogeneous after 0.1 Ma (Lameyre *et al.* 1976; Dosso *et al.* 1979). The 0.1-Ma period of time constitutes the maximum duration for emplacement, crystallization and cooling of a ring intrusion. Accordingly, the calculated rates of magma supply should be at least 0.03–0.07 $m^3 s^{-1}$, in the lowest range of values suggested by Petford *et al.* (2000). Taking these values gives a minimum sinking velocity of the subsiding block of 5 to 10 mm yr^{-1}.

Possible causes for cauldron subsidence In the Rallier-du-Baty nested ring complex, each unit records subsidence of the sinking block along a vertical distance ranging from 500 m to 1 km. If the subsided block is cylindrical, a space of the same order of magnitude should be open at depths. According to the geophysical evidence, currently active magma chambers contain a very limited quantity of liquid – less than 100–150 m thick. Thus, emptying of the top of the magma chamber by ascent of the residual liquid up to the ring complex level can accommodate only a small proportion of the observed vertical movement – implying a supplementary process.

We speculate that cauldron subsidence was accompanied by floor-depression of the underlying magma chamber. Basically, the density of a magma increases by *c.* 10% upon crystallization. A mafic magma, stalled in a magma chamber, may cool and evolve by fractional crystallization, as in the case for the Rallier-du-Baty area. Residual liquids yield lower densities, while denser cumulative rocks become negatively buoyant. If trapping occurs within the lower crust below the strength maximum, the crystallizing chamber can sink at velocities governed by the effective viscosity of the crust. Mafic plutons can sink at 0.5 to 50 mm yr^{-1} (Glazner 1994), consistent with the minimum sinking velocity of 5–10 mm yr^{-1} estimated for the subsiding block of the Rallier-du-Baty nested ring complex.

A relevant example is the Bjerkreim–Sokndal layered intrusion, Rogaland, Norway, where a thick sequence of cumulative mafic rocks is topped by an A-type silicic suite (Duchesne & Wilmart 1997). Magmatic fabrics are marked by mineral foliations and lineations converging and plunging into the centre of the massif. They are interpreted as resulting from centripetal gravitational collapse (Bolle 1998). Similarly, in the Coastal Batholith of Peru, floor subsidence could have occurred by foundering of crustal blocks into a deflating layer of partially melted rocks (Haederle & Atherton 2002).

Chemical modelling (Gagnevin *et al.* 2003) provides evidence that one kilogram of trachyte–syenite can be produced by differentiation of 5–6 kg of trachyandesite–trachybasalt, leaving 4–5 kg of cumulates, in agreement with the respective thicknesses of the ring complex and the underlying crust. We suggest, therefore, that the Rallier-du-Baty nested ring complex is underlain by a thick package of collapsed mafic chambers. A similar picture is revealed by geophysical imagery (reflection seismic, gravity and aeromagnetic data) in the African continent, where the 15-km wide Messum ring complex, Namibia, rests on top of a network of multiple intrusions of basaltic magmas (Bauer *et al.* 2003).

Summary and conclusions

The Rallier-du-Baty Peninsula is composed of Neogene to Recent volcanic and plutonic rocks. Four major episodes of magmatic activity have been identified:

1 Tertiary flood basalts were erupted during and/or before the Early Miocene and constitute plateaux that characterize the overall physiography of Kerguelen Archipelago. The volcanic pile, the base of which is now under sea-level, has an observed thickness of at least 1000 m. An extensive zeolitization event took place 15–12 Ma ago.

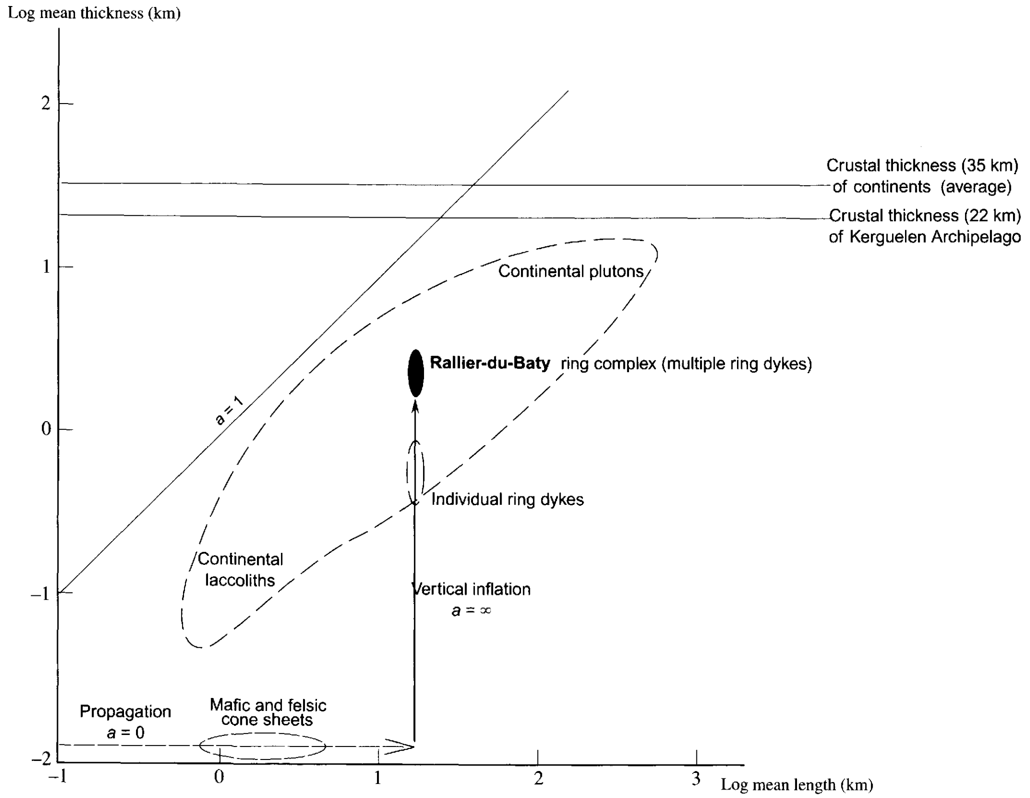

Fig. 12. Thickness v. length plot. Mafic and felsic cone sheets plot along a propagation trend ($a = 0$), individual ring dykes and the entire Rallier-du-Baty ring complexes plot along a vertical inflation trend ($a \rightarrow \infty$). Note that the oceanic Rallier-du-Baty ring complex yields dimensions of the same order of magnitude as continental intrusions, and plots in between laccoliths and plutons. Crustal thicknesses of continents and the Kerguelen Archipelago are shown for comparison.

2 Two ring complexes comprise early volcanic rocks intruded by younger plutonic rocks, both sharing quartz alkali-feldspar trachyte–syenite compositions. Remnants of a large caldera are preserved on the northern tip of the northern ring complex. The total volume of plutonic rocks is estimated at 400–800 km^3. If the volume of volcanic rocks emitted from the caldera is assumed to be of the same order of magnitude, each ring complex would correspond to the production of 800–1600 km^3 of magmatic rocks.

3 The Table-de-l'Institut caldera volcano is composed of trachyte, hawaiite and mugearite. The total volume of trachytic formations is estimated at more than 90 km^3. Hawaiite and mugearite products are comparatively more restricted in volume. The Table-de-l'Institut caldera volcano is likely to have erupted a total volume of 100 to 150 km^3. No plutonic equivalents have been found so far.

4 The Dôme Carva volcano is entirely composed of trachytic volcanic products, sharing hydro-plinian to plinian characteristics, culminating in voluminous ignimbrites and related pumice and ash falls. The Dôme Carva volcano is likely to have erupted a total volume of 25 to 30 km^3.

The plutonic ring complexes were emplaced through a two-stage mechanism involving: (1) horizontal elongation along a tensional fault plane, (2) vertical inflation aided by cauldron subsidence of a crustal block sinking into a deeper magma chamber along a cylindrical fault. They cross-cut a pre-existing caldera volcano, suggesting that the younger volcanoes themselves overlie unexposed ring complexes. Cooling of recent plutonic rocks induces the persistent fumarolic activity observed around Pic Saint-Allouarn.

Over the last 15 Ma, the volcanic and plutonic rocks of the Rallier-du-Baty Peninsula have recorded estimated volume 2800 ± 850 km^3 of magmas that passed up though the crust of the Rallier-du-Baty Peninsula. A residual volume of 1450 ± 450 km^3 of rocks is exposed, or inferred in the substratum, corresponding to a magmatically induced crustal thickening of 3.5 ± 1.0 km. It is only partly accommodated by the average elevation of 1000 m above the sea-level of the peninsula.

We are grateful to the French Institute for Polar Research and Technology (IFRTP), and especially to the Kerguelen technical staff for continuing support and assistance during the 1994–1995 Austral summer field expedition of the CARTOKER mapping project. The organizers of the LASI workshop at Freiberg: A. Mock, C. Breitkreuz and N. Petford, afforded a welcome opportunity for us to reconsider the role played by different mechanisms in the emplacement of one of the largest silicic ring complexes exposed in an oceanic island. Finally, thanks are due to R. Werner and L. Truelove for the astute comments in their reviews, and to the editors of the issue for their patience and efficient editorial handling of the manuscript.

References

ANDERSON, E.M. 1936. The dynamics of the formation of cone sheets, ring-dykes, and cauldron-subsidence. *Proceedings, Royal Society of Edinburgh*, **56**, 128–163.

AUBERT DE LA RUE, E. 1932. *Etude géologique et géographique de l'archipel de Kerguelen.* D.Sc. Thesis, Rev. Géogr. Phys. Géol. Dyn., **5**, 231 pp.

BAIN, A.D.N. 1934. The younger intrusive rocks of the Kudaru Hills, Nigeria. *Quarterly Journal of the Geological Society of London*, **90**, 201–239.

BAUER, K., TRUMBULL, R.B. & VIETOR, T. 2003. Geophysical images and a crustal model of intrusive structures beneath the Messum ring complex, Namibia. *Earth and Planetary Science Letters*, **216**, 65–80.

BELLAIR, P., CARRON, J.P., NOUGIER, J. & TRICHET, P. 1965. Niveaux intercalaires dans les strates de basalte des plateaux de l'Archipel de Kerguelen. *Geologische Rundschau*, **55**, 342–354.

BILLINGS, M.P. 1943. Ring-dikes and their origin. *New York Academy of Sciences, Transactions, Series. II*, **5**, 131–144.

BILLINGS, M.P. 1945. Mechanics of igneous intrusion in New Hampshire. *American Journal of Science, Daly Volume*, **243-A**, 40–68.

BOLLE, O. (1998). *Mélanges magmatiques et tectonique gravitaire dans l'apophyse de l'intrusion de Bjerkreim–Sokndal (Rogaland, Norvège): pétrologie, géochimie et fabrique magnétique.* Unpublished Ph.D. thesis, Université de Liège (Belgium), 204 pp.

BONIN, B. 1972. *Le complexe granitique subvolcanique de la région de Tolla-Cauro (Corse).* Ph.D. thesis, Université Pierre et Marie Curie, Paris, published by Lab. Géol. ENS, no. 7, 127 pp.

BONIN, B. 1986. *Ring Complex Granites and Anorogenic Magmatism.* Studies in Geology, North Oxford Academic Publications, Oxford, 188 pp.

CHARVIS, P., RECQ, M., OPERTO, S. & BREFORT, D. 1995. Deep structure of the northern Kerguelen plateau and hotspot-related activity. *Geophysical Journal International*, **122**, 899–924.

CHRISTIANSEN, R.L. & BLANCK, H.R. JR 1972. Volcanic stratigraphy of the Quaternary rhyolite plateau in Yellowstone National Park. *US Geological Survey Profession Paper*, **729-B**, 18 pp.

CLARKE, D.B., HENRY, A.S. & WHITE, M.A. 1998. Exploding xenoliths and the absence of 'elephant's graveyards' in granite batholiths. *Journal of Structural Geology*, **20**, 1325–1343.

CLOUGH, C.T., MAUFE, H.B. & BAILEY, E.B. 1909. The cauldron-subsidence of Glen Coe, and the associated igneous phenomena. *Quarterly Journal of the Society of London*, **65**, 611–678.

CORRY, C.E. 1988. Laccoliths: mechanics of emplacement and growth. *Geological Society of America Special Publications*, **220**, 110 pp.

CRUDEN, A.R. 1998. On the emplacement of tabular granites. *Journal of the Geological Society of London*, **155**, 853–862.

CRUDEN, A.R. & MCCAFFREY, K.J.W. 2001. Growth of plutons by floor subsidence: implications for rates of emplacement, intrusion spacing and melt-extraction mechanisms. *Physics and Chemistry of the Earth A*, **26**, 303–315.

DELORME, H., VERDIER, O., CHEMINÉE, J.L., GIRET, A., PINEAU, F. & JAVOY, M. 1994. Etude chimique et rapport isotopique du carbone des fumerolles de la péninsule Rallier du Baty (îles Kerguelen). *In*: SCHLICH, R. & GIRET, A. (eds), *Géologie et géophysique des Kerguelen*, Mémoires de la Société Géologique de France, Nouvelle Série, **166**, 25–30.

DOSSO, L., VIDAL, P., CANTAGREL, J.M., LAMEYRE, J., MAROT, A. & ZIMINE, S. 1979. 'Kerguelen: continental fragment or oceanic island?': petrology and geochemistry evidence. *Earth and Planetary Science Letters*, **43**, 46–60.

DOSSO, L. & MURTHY, V.R. 1980. A Nd isotopic study of the Kerguelen Islands: inferences on enriched oceanic mantle sources. *Earth and Planetary Science Letters*, **48**, 268–276.

DUCHESNE, J.C. & WILMART, E. 1997 Igneous charnockites and related rocks from the Bjerkreim–Sokndal layered intrusion (Southwest Norway): a jotunite (hypersthene monzodiorite)-derived A-type granitoid suite. *Journal of Petrology*, **38**, 337–369.

GAGNEVIN, D. *ET AL.* 2003. Open-system processes in the genesis of silica-oversaturated alkaline rocks of the Rallier-du-Baty peninsula, Kerguelen Archipelago (Indian Ocean). *Journal of Volcanology and Geothermal Research*, **123**, 267–300.

GEOFFROY, L., OLIVIER, P. & ROCHETTE, P. 1997. Structure of a hypovolcanic acid complex inferred from magnetic susceptibility anisotropy measurements: the Western Red Hills granites (Skye, Scotland, Thulean Igneous Province). *Bulletin of Volcanology*, **59**, 147–159.

GIRET, A. 1980. *Notice et carte géologique au 1:50 000 de la Péninsule Rallier du Baty, Iles Kerguelen.* CNFRA, **45**, 14 pp.

GIRET, A. 1990. Typology, evolution, and origin of the Kerguelen plutonic series, Indian Ocean: a review. *Geological Journal*, **25**, 239–247.

GIRET, A. 1993. Les étapes magmatiques de l'édification des îles Kerguelen, océan Indien. *Mémoire de la Société Géologique de France*, **163**, 273–282.

GIRET, A., VERDIER, O. & NATIVEL, P. 1992. The zeolitisation model of Kerguelen Islands, Southern Indian Ocean. *In*: YOSHIDA, Y. *et al.* (eds), *Recent Progress in Antarctic Earth Science*, TERRAPUB, Tokyo, 457–463.

GIRET, A., GRÉGOIRE, M., COTTIN, J.Y. & MICHON, G. 1997. Kerguelen, a third type of oceanic island? *In*: RICCI, C.A. (ed.) *The Antarctic Region: Geological Evolution and Processes.* Terra Antarctica Publication, 735–741.

GLAZNER, A.F. 1994. Foundering of mafic plutons and density stratification of continental crust. *Geology*, **22**, 435–438.

GRÉGOIRE, M., COTTIN, J.Y., GIRET, A., MATTIELLI, N. & WEIS, D. 1998. The meta-igneous granulite xenoliths from Kerguelen Archipelago: evidence of a continent nucleation in an oceanic setting. *Contributions to Mineralogy and Petrology*, **133**, 259–283.

HAEDERLE, M. & ATHERTON, M.P. 2002. Shape and intrusion style of the Coastal Batholith, Peru. *Tectonophysics*, **345**, 17–28.

KINGSLEY, L. 1931. Cauldron-subsidence of the Ossipee Mountains. *American Journal of Science, 5th Series*, **22**, 139–168.

LACROIX, A. 1922. *Minéralogie de Madagascar.* Challamel, Paris, Vol. 2, 694 pp.

LACROIX, A. 1924. Les roches éruptives grenues de l'archipel de Kerguelen. *Comptes Rendus de l'Académie des Sciences, Paris*, **179**, 113–119.

LAMEYRE, J., MAROT, A., ZIMINE, S., CANTAGREL, J.M., DOSSO, L. & VIDAL, P. 1976. Chronological evolution of the Kerguelen islands syenite–granite ring complex. *Nature*, **263**, 306–307.

LAMEYRE, J. ET AL. 1981. *Etude Géologique du Complexe Plutonique de la Péninsule Rallier du Baty, Iles Kerguelen.* CNFRA, **49**, 176 pp.

LEYRIT, H. 1992. *Kerguelen: cartographie et magmatologie des presqu'îles Jeanne d'Arc et Ronarc'h.* Ph.D. thesis, Université de Paris-Sud, Orsay, 236 pp.

MCCAFFREY, K.J.W. & PETFORD, N. 1997. Are granitic intrusions scale invariant? *Journal of the Geological Society of London*, **154**, 1–4.

MAROT, A. & ZIMINE, S. 1976. *Les complexes annulaires de syénites et granites alcalins dans la péninsule Rallier du Baty, Iles Kerguelen (T.A.A.F).* Ph.D. thesis, Université Pierre et Marie Curie, Paris, 172 pp.

MARTIN, R.F. & BONIN, B. 1976. Water and magma genesis: the association hypersolvus granite–subsolvus granite. *Canadian Mineralogist*, **14**, 228–237.

MUNSCHY, M., FRITSCH, B., SCHLICH, R. & ROTSTEIN, Y. 1994. Tectonique extensive sur le plateau de Kerguelen. *In*: SCHLICH, R. & GIRET, A. (eds), *Géologie et Géophysique des Kerguelen*, Mém. Soc. Géol. Fr., N.S., **166**, 99–108.

NOUGIER, J. 1970. *Contribution à l'étude Géologique et Géomorphologique des Iles Kerguelen.* CNFRA, **27(1)**, 440 pp., **27(2)**, 246 pp.

ORCEL, J. 1924. Notes minéralogiques et pétrographiques sur la Corse. *Bulletin de la Société des Sciences Historiques et Naturelles de la Corse, Bastia*, **461–464**, 65–127.

PETFORD, N., CRUDEN, A.R., MCCAFFREY, K.J.W. & VIGNERESSE, J.L. 2000. Granite magma formation, transport and emplacement in the Earth's crust. *Nature*, **408**, 669–673.

RECQ, M., LE ROY, I., CHARVIS, P., GOSLIN, J. & BREFORT, D. 1994. Structure profonde du Mont Ross d'après la sismique (îles Kerguelen, océan Indien austral). *Canadian Journal of Earth Sciences*, **31**, 1806–1821.

RICHEY, J.E. 1928. The structural relations of the Mourne Granites (Northern Ireland). *Quarterly Journal of the Geological Society of London*, **83**, 653–687.

RICHEY, J.E. 1932. Tertiary ring structures in Britain. *Transactions of the Royal Society of Glasgow*, **19**, 42–140.

RICHEY, J.E. 1935. *Scotland: the Tertiary Volcanic Districts. British Regional Geology*, HMSO, Edinburgh, 120 pp.

ROCCHI, S., WESTERMAN, D.S., DINI, A., INNOCENTI, F. & TONARINI, S. 2004. Two-stage laccolith growth at Elba Island (Italy). *Geology*, in press.

SCHLICH, R. 1994. Introduction. *In*: SCHLICH, R. & GIRET, A. (eds), *Géologie et Géophysique des Kerguelen*, Mémoires de la Société Géologique de France, Nouvelle Série, **166**, 5–6.

SCHUBERT, G. & SANDWELL, D. 1989. Crustal volumes of the continents and of oceanic and continental submarine plateaus. *Earth and Planetary Science Letters*, **92**, 234–246.

VERDIER, O. 1989. *Champs géothermiques et zéolitisation des îles Kerguelen: implications géologiques (Terres Australes et Antarctiques Françaises, Océan Indien Austral).* Ph.D. thesis, Université Pierre et Marie Curie, Paris, 271 pp.

WEIS, D., FREY, F.A., GIRET, A. & CANTAGREL, J.M. 1998. Geochemical characteristics of the youngest volcano (Mount Ross) in the Kerguelen Archipelago: inferences for magma flux, lithosphere assimilation and composition of the Kerguelen Plume. *Journal of Petrology*, **39**, 973–994.

YANG, H.-J., FREY, F.A., WEIS, D., GIRET, A., PYLE, D. & MICHON, G. 1998. Petrogenesis of the flood basalts forming the northern Kerguelen Archipelago: implications for the Kerguelen Plume. *Journal of Petrology*, **39**, 711–748.